2003.6.13

Kondo effect in mesoscopic systems

(experimetal)

엄 종 화

세종대학교 물리학과

(http://dasan.sejong.ac.kr/~eom/)

Kondo effect in mesoscopic systems (experimental)

I. Kondo effect in mesoscopic metallic alloys

(1) Finite size effect in Kondo alloys

(2) Thermopower of mesoscopic spin glasses

(3) Superconducting proximity effect in Kondo alloys

II. Kondo effect in low-dimensional systems

(1) Kondo effect in a single electron transistor

(2) Kondo effect in carbon nanotubes

(3) Kondo effect in a single molecule transistor

Kondo model

Dilute Magnetic Alloy

Single localized spin impurity embedded in s-like electron sea

; AuFe, AuMn, CuFe, CuMn, CuCr …..

$$H = \sum_{k,\sigma} \varepsilon_k c^+_{k\sigma} c_{k\sigma} + \varepsilon_L (n_{L\uparrow} + n_{L\downarrow}) + H_{sd}$$

Conduction electrons　　Localized d-electron　　s-d exchange interaction

; formulated by Zener(1951), and Kondo showed(1964) the spin-flip scattering could cause unusual low-temperature behavior by going beyond first Born approximation.

impurity spin

$$H_{sd} = -J_{s-d}\, \vec{S} \cdot \vec{s}$$

conduction spin

$$= -\frac{1}{2N} \sum_{k,q} J_{kq} [S_L^{(z)} (c^+_{k+q\uparrow} c_{k\uparrow} - c^+_{k+q\downarrow} c_{k\downarrow}) + S_L^{(+)} c^+_{k+q\downarrow} c_{k\uparrow} + S_L^{(-)} c^+_{k+q\uparrow} c_{k\downarrow}]$$

Non spin-flip process : H^z_{sd}　　spin flip process : $H^{\pm}_{sd}$

LogT dependence in R(T)

Scattering amplitude for a channel of $k\uparrow \Rightarrow k'\uparrow$

$$\boxed{t_{k\uparrow,k'\uparrow} = t_{k\uparrow,k'\uparrow}{}^{(1)} + t_{k\uparrow,k'\uparrow}{}^{(2)} + \cdots}$$

$$t^{(1)}_{k\uparrow,k'\uparrow} = -\frac{J}{2N} S_z$$

$$t^{(2)}_{k\uparrow,k'\uparrow} = t^{(2)}_{k\uparrow,k'\uparrow}\Big|_z + t^{(2)}_{k\uparrow,k'\uparrow}\Big|_\pm = 0 - 2\left(\frac{J}{2N}\right)^2 S_z N(0)\ln(kT/D)$$

where N : number of d-electrons, N(0) : density of state at E_F

D : width of conduction electron distribution around E_F

$$\begin{aligned} J_{k,q} &= J \quad \text{where } -D < \varepsilon_k, \varepsilon_q < D \\ &= 0 \quad \text{otherwise} \end{aligned}$$

$$\boxed{R_{Kondo}(T) \propto c\,\frac{2\pi}{\hbar}\left|t_{k\uparrow,k\uparrow}\right|^2 = c\,R_m\left[\,1 + \frac{2J}{N} N(0)\ln(kT/D) + \ldots\,\right]}$$

This $\ln T$ dependence combined with the phonon contribution (T^5 dependence) makes a resistance minimum in R(T).

Anderson model

$$H = \sum_{k,\sigma} \varepsilon_k c^{+}_{k\sigma} c_{k\sigma} + \varepsilon_L (n_{L\uparrow} + n_{L\downarrow}) + \sum_{k\sigma} M_k (c^{+}_{k\sigma} c_{L\sigma} + c^{+}_{L\sigma} c_{k\sigma}) + U n_{L\uparrow} n_{L\downarrow}$$

Mixing term

Coulomb interaction

Fano-Anderson model

Mixing term : process where electron hops off of the impurity and becomes a continuum state and vise versa.

Coulomb interaction causes interesting magnetic phenomena.

Anderson model and Kondo model both describe the interaction of a continuum electron with localized electron. The two models are not totally different. There is a canonical transformation which when applied to the Anderson model will transform it into a form similar to the Kondo model. This transformation on the Anderson model produces quite a few terms, of which the Kondo model is a subset. Thus the transformation does not produce exactly the Kondo model. Thus the transformation does not produce exactly the Kondo model, and the two models are not identical.
- Gerald D. Mahan, Many-Particle Physics (Plenum, 1993)

LogT dependence of Kondo resistivity

Loram et al., PRB 2, 857 (1970)

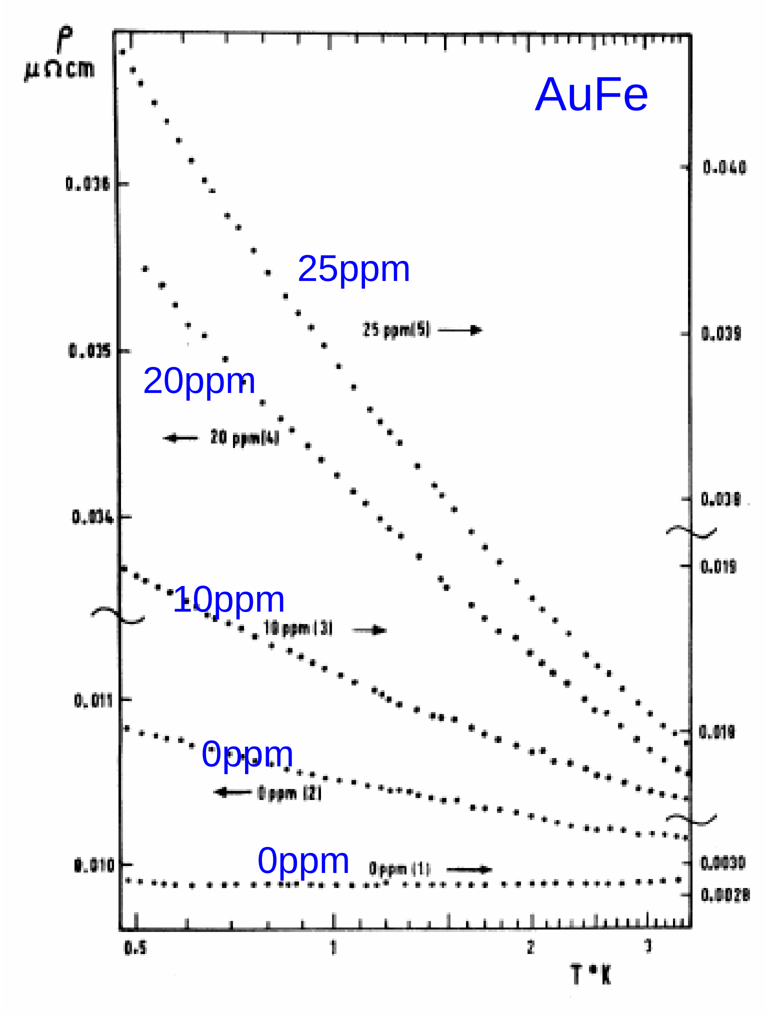

FIG. 2. $\rho\,\mu\Omega$cm against $\log_{10}T$ for very dilute *Au*Fe alloys. Nominal Fe concentration in each alloy is show in ppm Fe and the specimen number in this and subsequent figures is shown in parentheses.

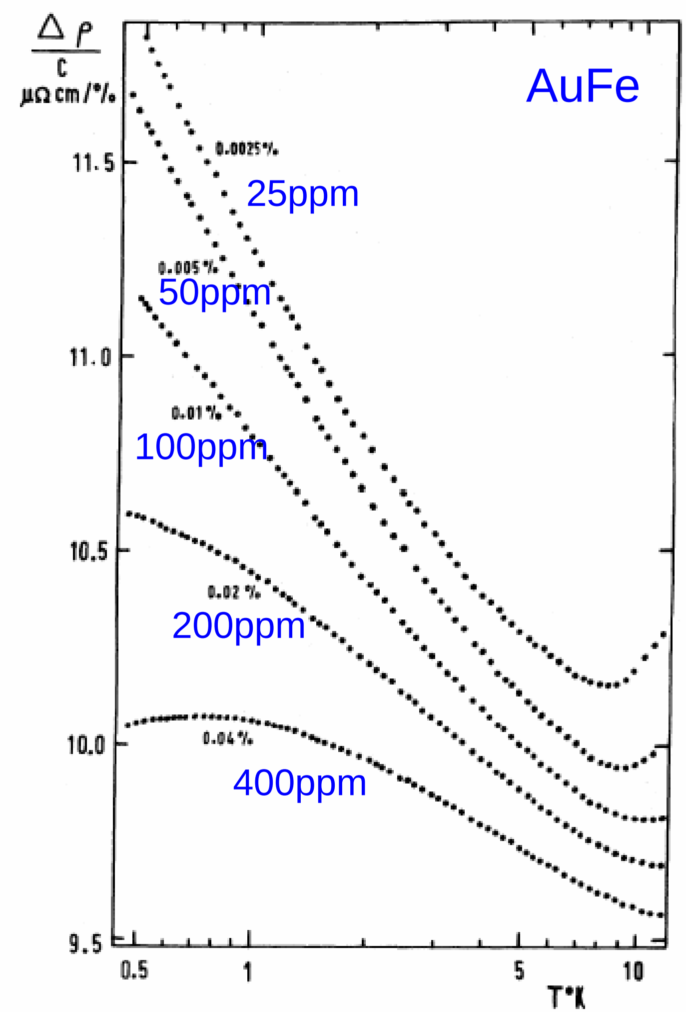

FIG. 3. $(\Delta\rho/c)\mu\Omega$cm/at. % against $\log_{10}T$ for more concentrated *Au*Fe alloys. Nominal Fe concentration is indicated for each alloy.

Temperature dependence around T_K

Kondo effect in resistivity, $\rho(T)$

When $T \ll T_K$, $\rho \sim (\rho_0 - cT^2)$: Unitary limit

When $T_K \ll T$, $\rho \sim \log(T/T_K)$

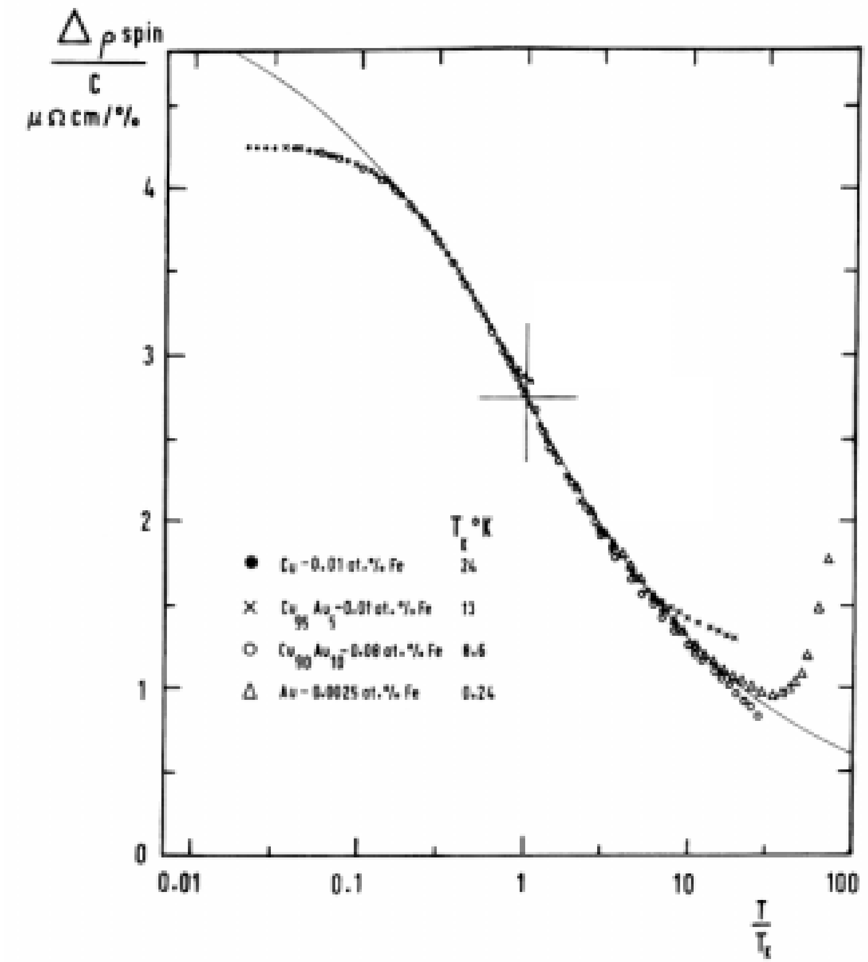

When $T \sim T_K$

Hamann expression for Kondo resistivity

Hamann, Phys. Rev. 158, 570 (1967)

$$\Delta\rho(T) \propto \frac{1}{2}\rho_0\left(1 \pm \left[1 + \frac{S(S+1)\pi^2}{[\ln(T/T_K)]^2}\right]^{-\frac{1}{2}}\right)$$

$T_K > T$ 일 때, 수식에서 (-) 부호,

$T_K < T$ 일 때, 수식에서 (+) 부호를 취한다.

여기서, ρ_0 는 자성물질의 농도에 비례한다.

From fitting, T_K is obtained

여러 가지 물질의 Kondo temperatures

$T_K \sim T_F \exp[-1/\{J\,N(0)\}]$

여기서 J : s-d exchange coupling, N(0) : conduction electron density of states

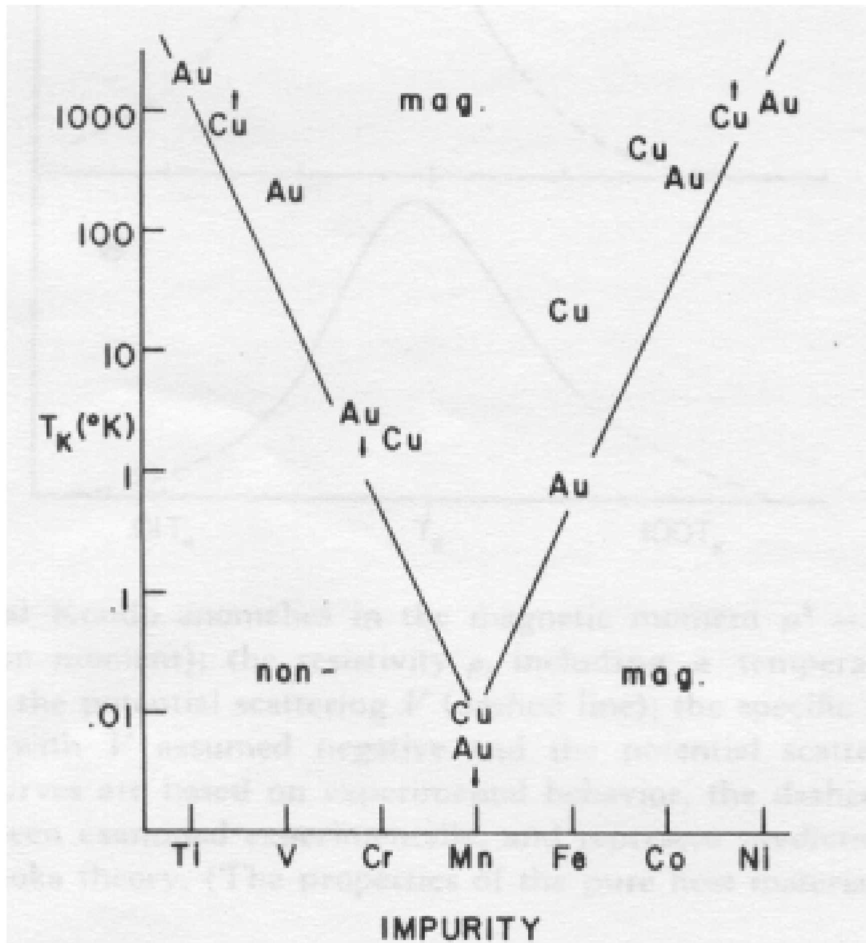

Size of the Kondo screening cloud: the Kondo length

Simple picture

Kondo effect arises from the screening of moment of a magnetic impurity by the conduction electrons in the host metal.

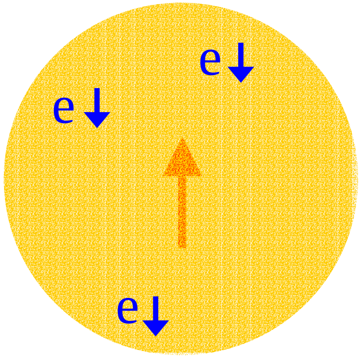

spin singlet state

Size of the Kondo screening cloud : $\xi_K \approx \dfrac{\hbar \upsilon_F}{kT_K}$

For AuFe with T_K ~ 1 K, ξ_K ~ 10 μm

If the Kondo screening cloud is distorted by reducing the sample dimension, the Kondo effect may be suppressed.

The first observation of size dependence of Kondo effect

Chen and Giordano, PRL 66, 209 (1991)

AuFe(30ppm) 2D film

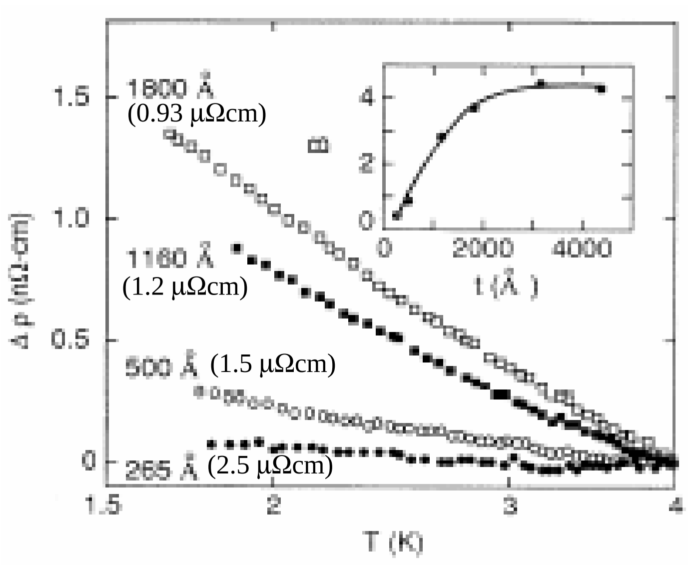

$$\Delta\rho = -B \ln T$$

The coefficient B depends on thickness, t.

박막두께가 얇아질수록 kondo slope은 감소한다.

$$\xi_K \approx \frac{\hbar v_F}{kT_K} = 10\ \mu m \quad \text{where } T_K \sim 1\text{K}$$

Au/AuFe (110 A / 250 A)

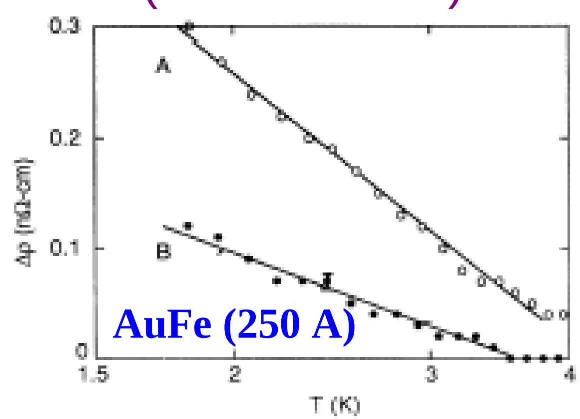

Kondo screening cloud can expand to the adjacent Au layer

Finite size effect in Kondo alloys

CuCr(1000ppm) wire

DiTusa et al., PRL 68, 678 (1992)

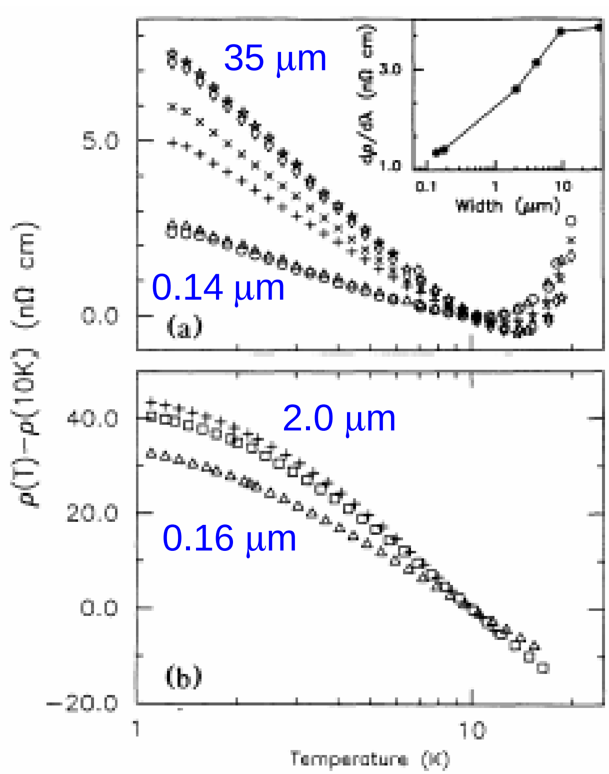

(a) 21.2 nm thick film

$$\frac{d\rho}{d(\ln T\,/\,T_K)} \quad \text{vs. width}$$

w = 0.14, 0.16, 2, 4, 9.5, 35 μm

(b) 98 nm thick film

w = 0.16, 0.76, 2 μm

선폭이 감소할수록 kondo slope은 감소한다.

(c) 20 nm thick CuCr(2000ppm) film

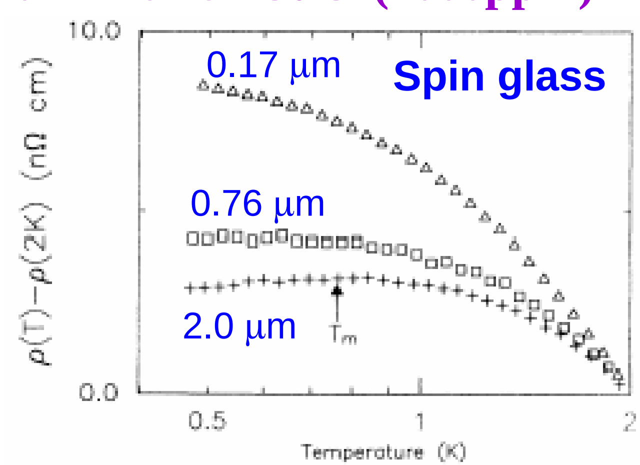

선폭이 감소할수록 inter-spin interaction 이 감소한다.

Finite size effect in Kondo alloys

AuFe(70ppm) wire

Blachly and Giordano et al., PRB 46, 2951 (1992)

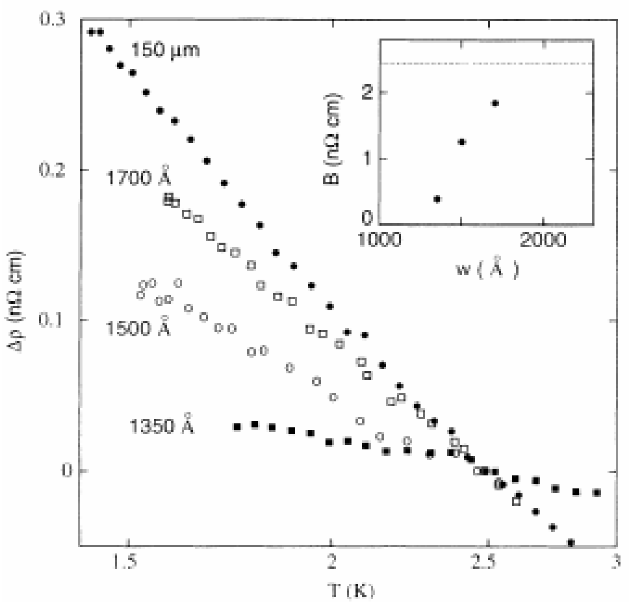

15 nm thick film

Slope decreases as width(w) is decreased.

선폭이 감소할수록 kondo slope은 감소한다.

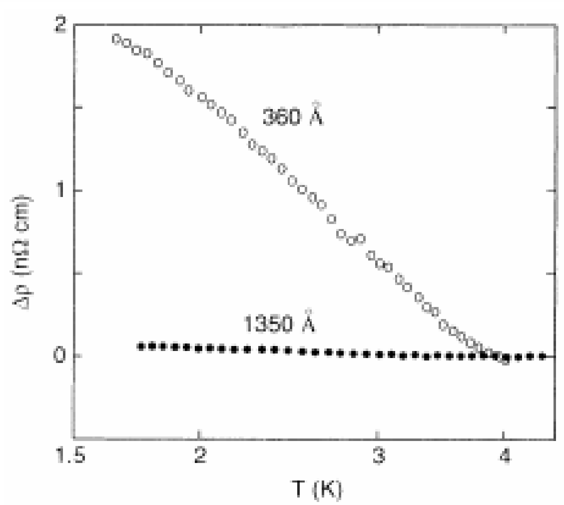

Δρ increases as w is decreased below 1350 A.

The δρ by e-e intreraction becomes important in 1-D.

$$\delta\rho_{ee}^{(1)} = A_1 \frac{R_S^2 \, t}{(\pi\hbar / e^2) w} L_T = A_1 \frac{R_S^2 \, t}{(\pi\hbar / e^2) w} \sqrt{\frac{\hbar D}{kT}}$$

where $A_1 \sim 1.56$

Mechanically controllable break junction: A useful tool for size effect study

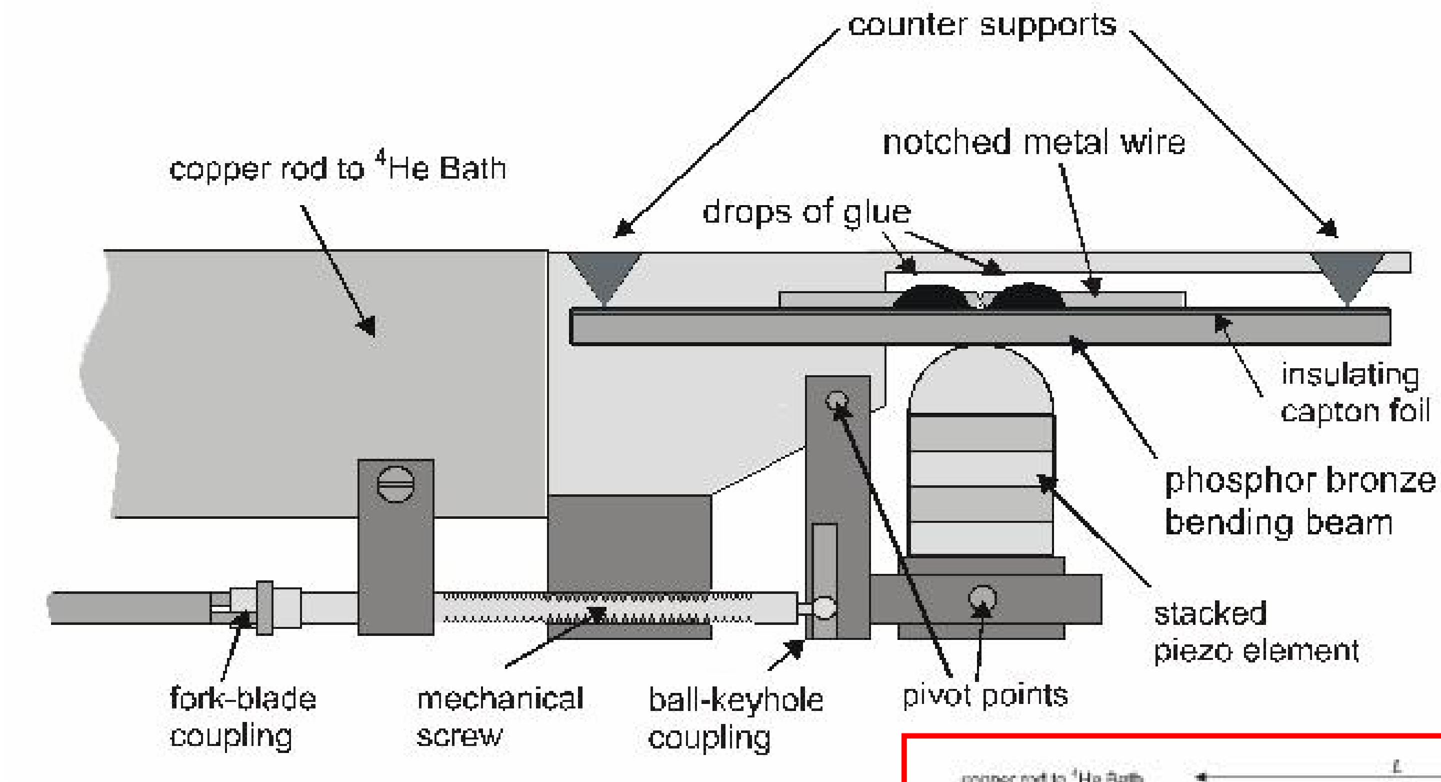

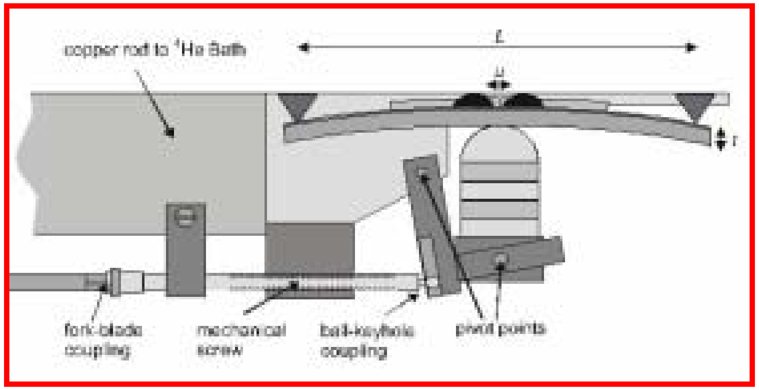

The diameter of the contact is given by Sharvin relation for ballistic contacts

(Yanson, Sov. J. Low Temp. Phys. 9, 343 (1983))

$$k_F d = \sqrt{\frac{8h}{e^2 R}} \qquad \left(for \;\; Cu, \quad d[nm] = \frac{30}{\sqrt{R[\Omega]}} \right)$$

Mechanically controllable break junction

CuMn (1000ppm)

Yanson et al., PRL 74, 302 (1995)

Point contact spectroscopy

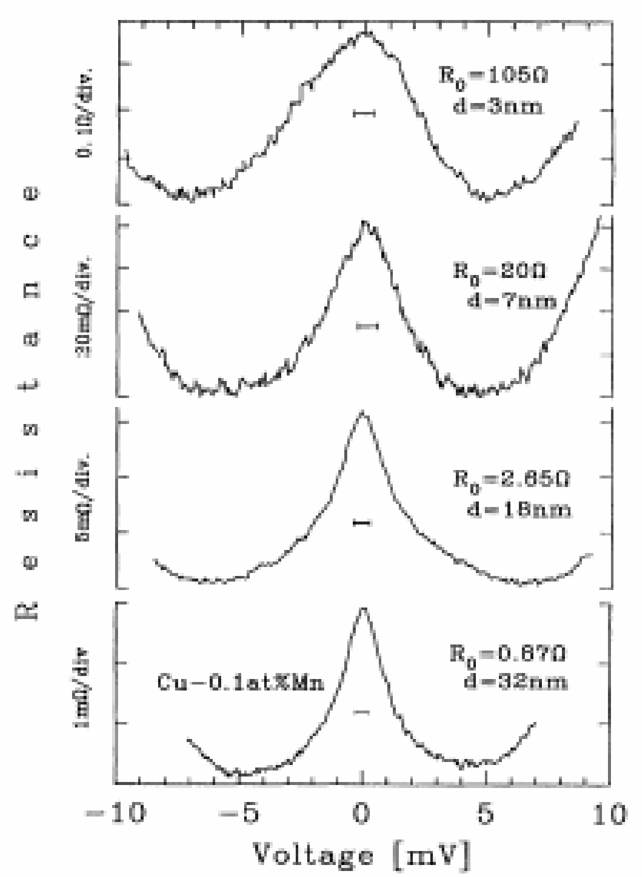

$$\frac{\delta R_K}{R_0} \approx 0.003 \text{ for all contact size}$$

In second-order Born approximation the magnetic impurity contribution to the point contact spectroscopy

Omelyanchuk, Sov. J. Low. Temp. Phys. 11, 211 (1985).

$$-\frac{d^2 I}{dV^2} \approx Q\frac{1}{V} \quad (when\ \ eV >> kT)$$

$$\text{where} \quad Q = \frac{105}{8} c \frac{k_F d}{R_0}\left(\frac{J}{E_F}\right)^3 \qquad for \quad S(Mn) = 5/2$$

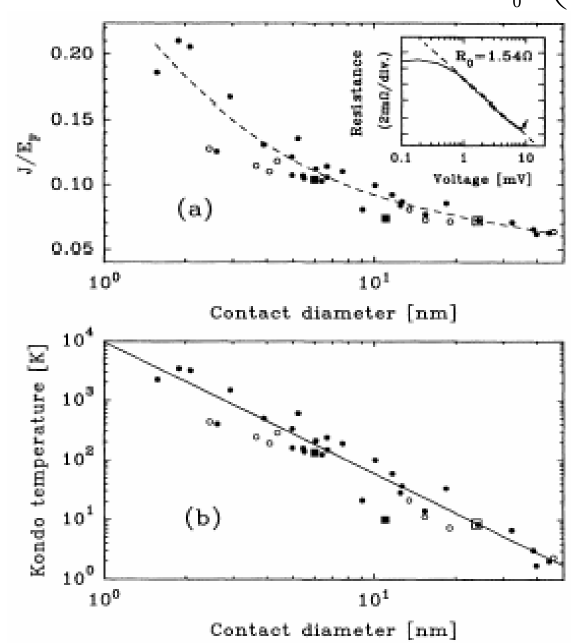

$$\frac{J}{E_F} = -0.044\left(\frac{1}{c\sqrt{R_0}} \frac{dR}{d\log_{10} V}\right)^{1/3}$$

c : impurity concentration

$$kT_K = E_F \exp\left(-\frac{2}{3J/E_F}\right)$$

Size가 작아질수록 kondo 온도는 증가한다.

Absence of size dependence of the Kondo resistivity

AuFe (50ppm)

Chandrasekhar et al., PRL 72, 2053 (1994)

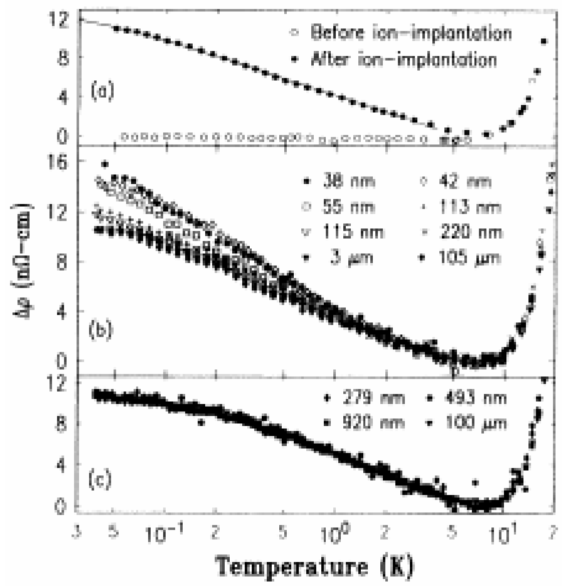

Slope increases as the width decreases.

Slope increase is not appreciable when w > 300 nm.

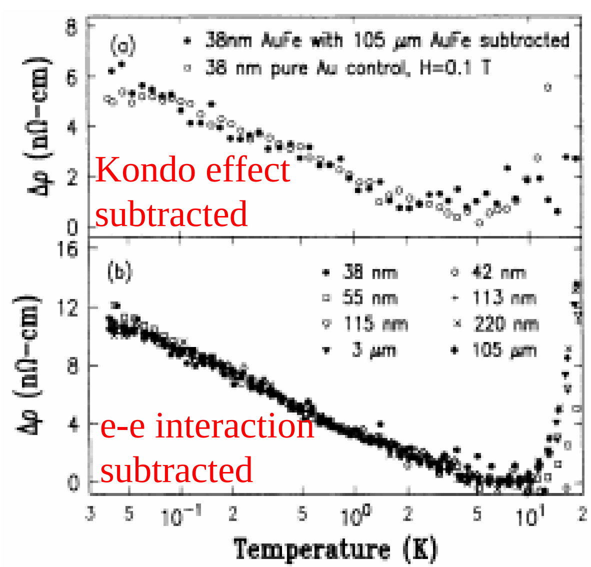

Contributions to the low temp resistivity

1. Kondo effect
2. e-e interaction (width dependence in 1-D wires)
3. weak localization (negligible in magnetic sample)

For 1-D system, $$\Delta\rho_{ee}(T) = \alpha \frac{R_S^2 t}{(\pi\hbar / e^2) w} L_T$$

; Altshuler and Aronov, *Electron-electron interactions in disordered systems* (1985)

No size dependence of Kondo resistivity

Size dependence in the spin-glass resistivity of AuFe wires

AuFe (0.28%, 0.85%)

Neuttiens et al., Europhy. Lett. 34, 617 (1996)

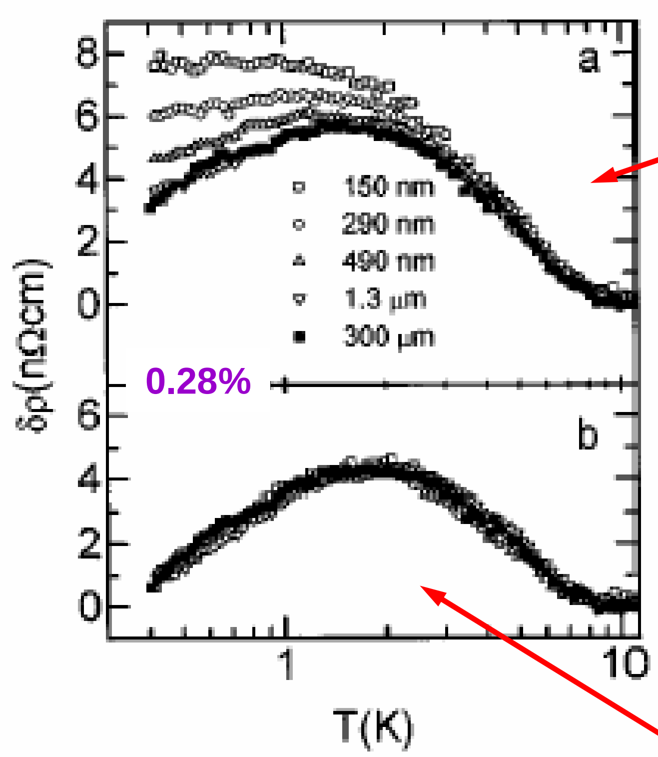

Raw data

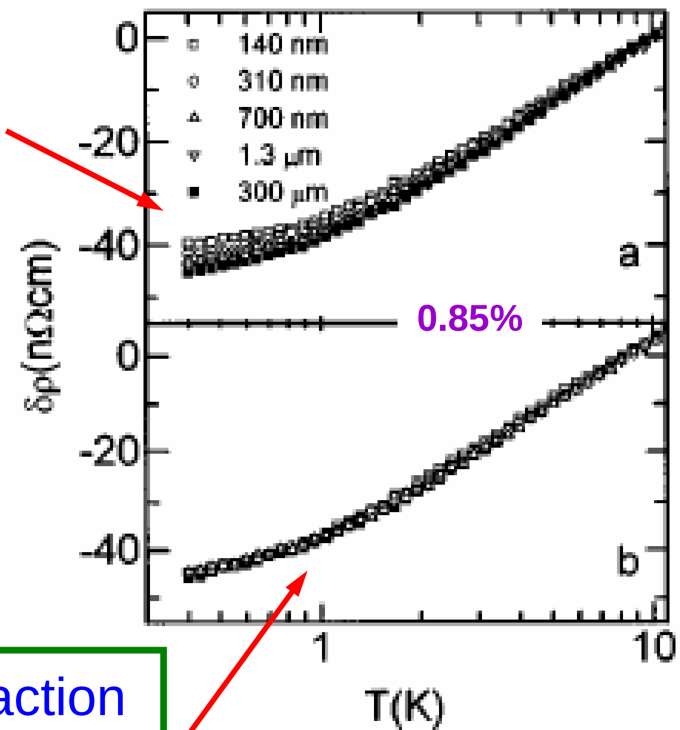

After e-e interaction subtracted

No size dependence of spin-glass resistivity

Theoretical models for the finite size dependence in the Kondo effect

Spin-orbit interaction gives rise to size dependent magnetic anisotropy.

; Ujsaghy et al., PRL 76, 2378 (1996)

The volume to surface ratio of samples is important factor.

In a disordered samples, weak localization can lead to a finite size dependence in the Kondo resistivity.

; Martin et al., PRL 78, 114 (1997)

It is obviously interesting to look at other transport properties which are affected by the spin scattering.

→ thermopower (thermoelectric power)

Mott's formula directly reflects the pronounced energy dependence of the scattering time induced by the magnetic impurity.

; Barnard, *Thermoelectricity in Metals and Alloys* (Taylor & Francis, London, 1972)

Kondo, Spin glass, Ferromagnet

Noble metal (Au, Ag, Cu, …) + Magnetic impurity (Fe, Cr, Mn, …)

AuFe

순수 귀금속류 : Au

Kondo sample : Au + Fe (0.04% 이하) T_K = 0.3 ~ 0.8 K

Spin glass : Au + Fe (0.04% ~ 10%) T_g= 1 ~ 10 K

Inhomogeneous Ferromagnet : Au + Fe (10% 이상) T_0 > 30 K

Metallic Spin Glass

Magnetization of a free electron gas
by RKKY interaction

$$J_{RKKY}(r) \propto \frac{1}{r^2}\left[\frac{\cos k_F r}{2k_F r} - \frac{\sin k_F r}{(2k_F r)^2}\right]$$

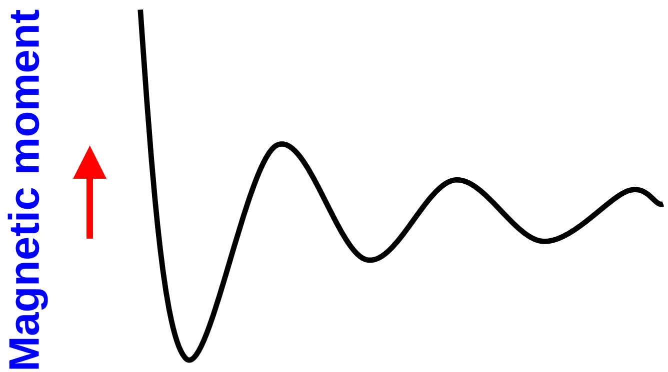

In disordered metal ($r > l_e$) (Jagannathan et al.,PRB 37, 436 (1998).)

$$J(r) \propto J \exp(-r / l_e) + 3\left(\frac{mk_F}{8\pi^3}\right)^2 \frac{1}{r^6}$$

Spins freeze in random directions below T_g .

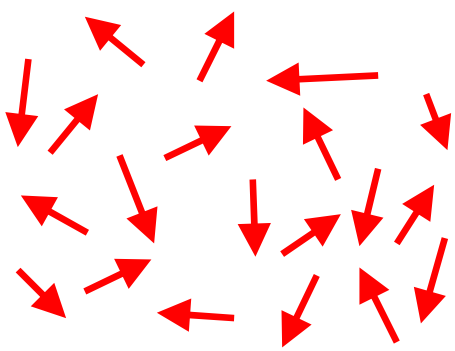

- Broad peak in R(T), c(T)
- Sharp peak in c(T)
- Hysteresis and Remanent Magnetization
- No long-range order

Thermopower of AuFe

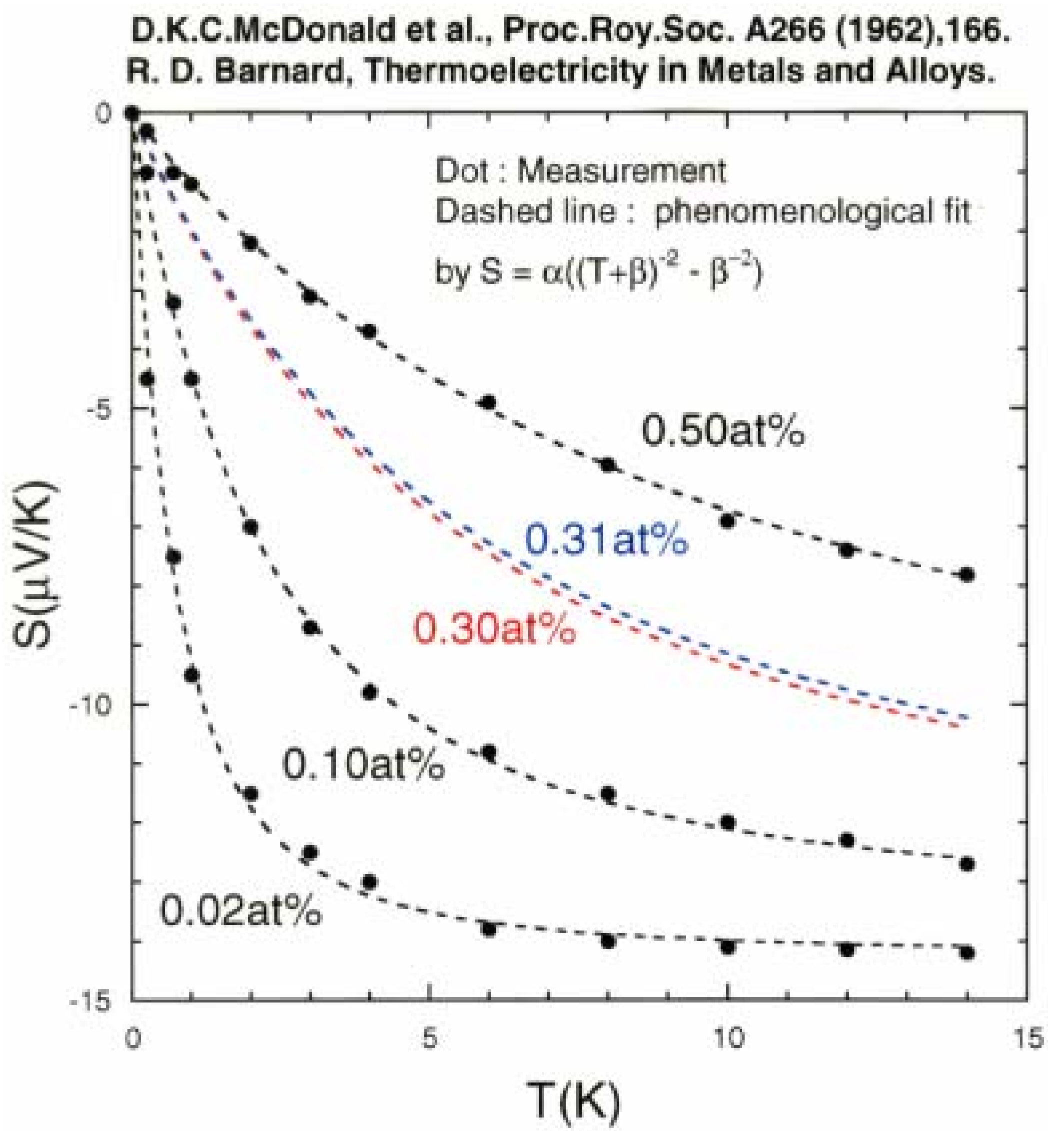

Differential resistance of AuFe spin glass

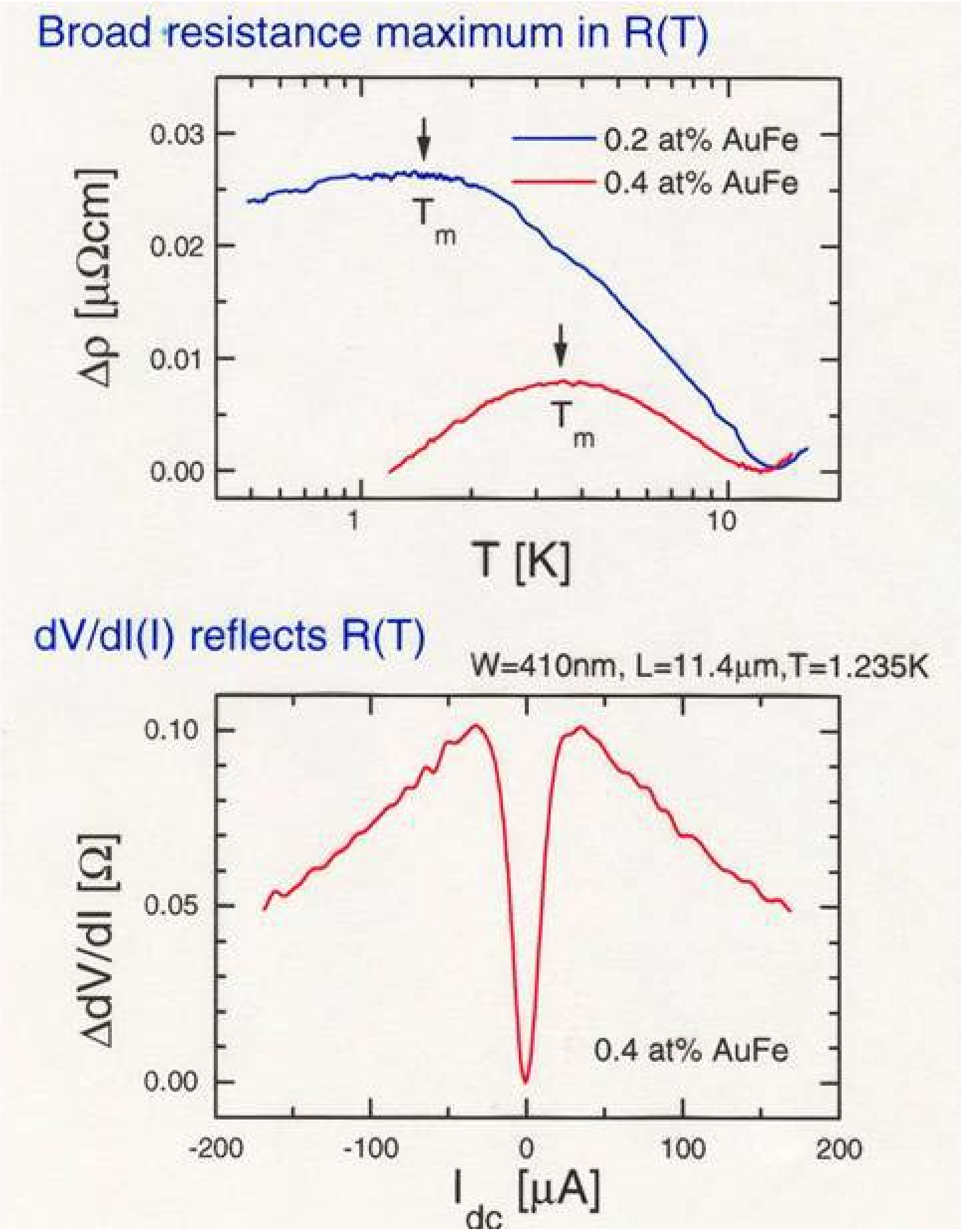

Eom et al., PRL (1996)

Broad resistance maximum.

T_m increases as c increases.

Differential resistance, dV/dI(I)

I 와 매우 작은 I_{ac}를 샘플에 흘려주고 I_{ac}의 frequency에 해당하는 response를 측정한다. (Lock amplifier 이용)

← I 방향에 관계없이 symmetric

Asymmetric dV/dI of AuFe wire

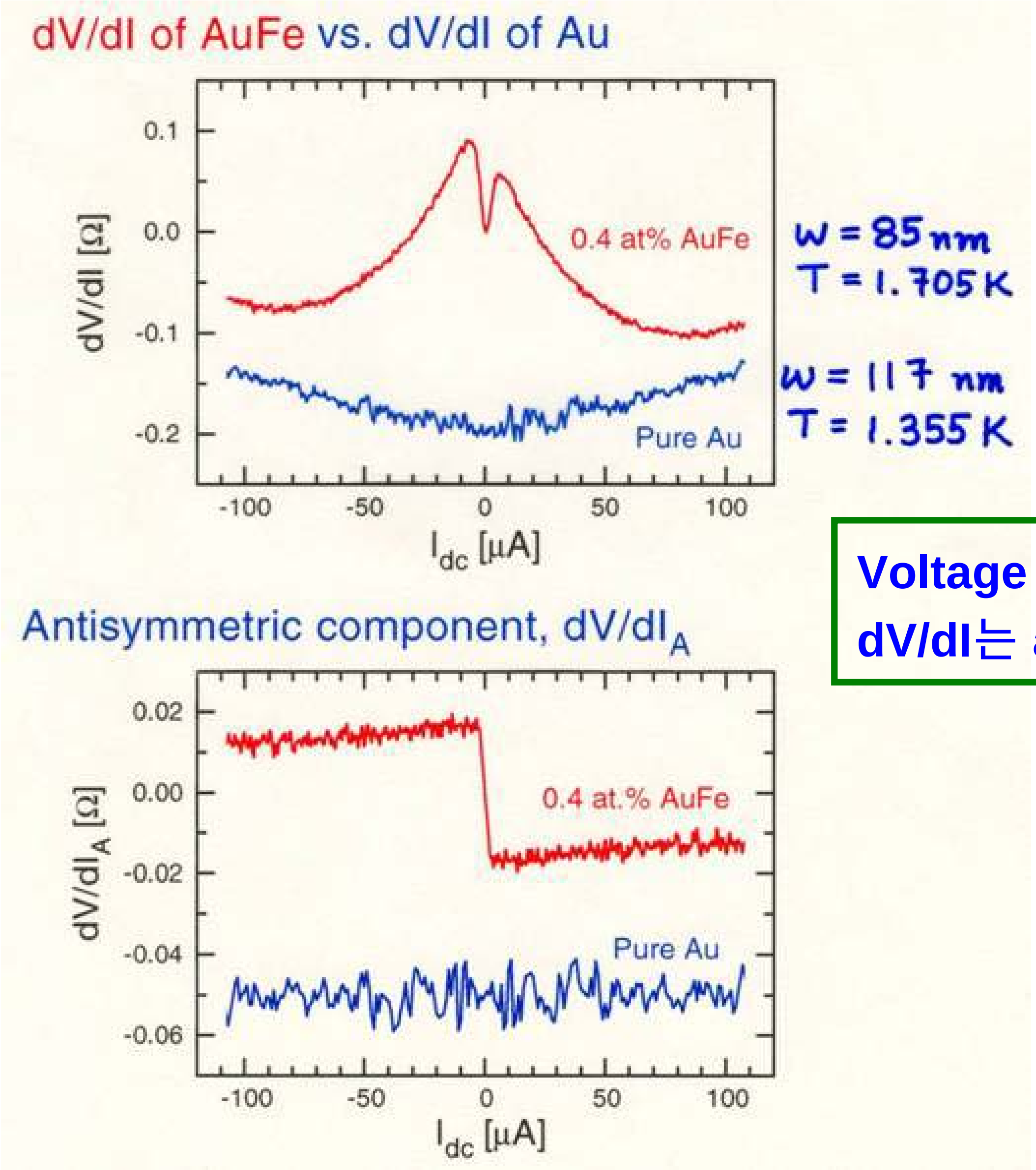

Voltage probe의 width가 서로 다를 때 dV/dI는 asymmetric하게 나온다.

Antisymmetric part of dV/dI

AuFe(0.3%) film thickness = 30 nm

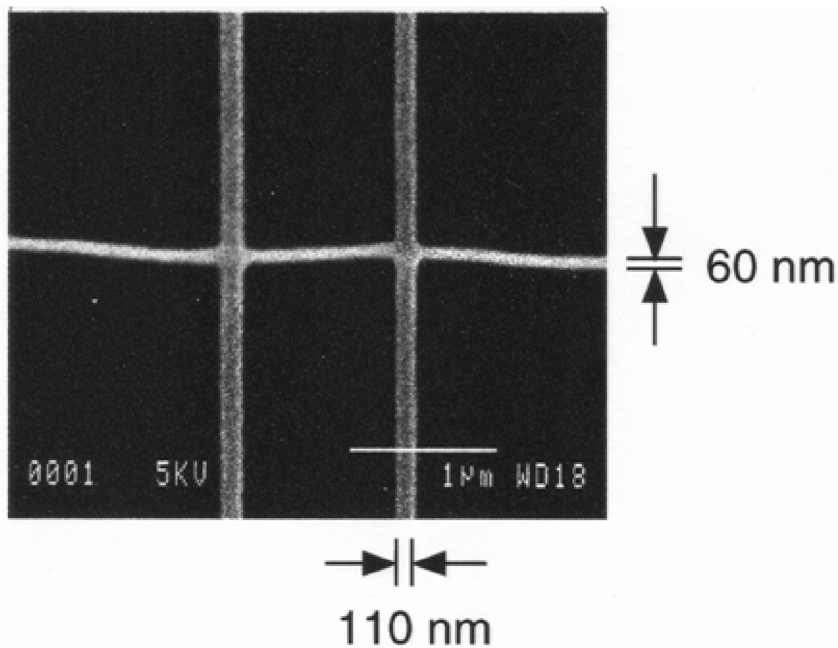

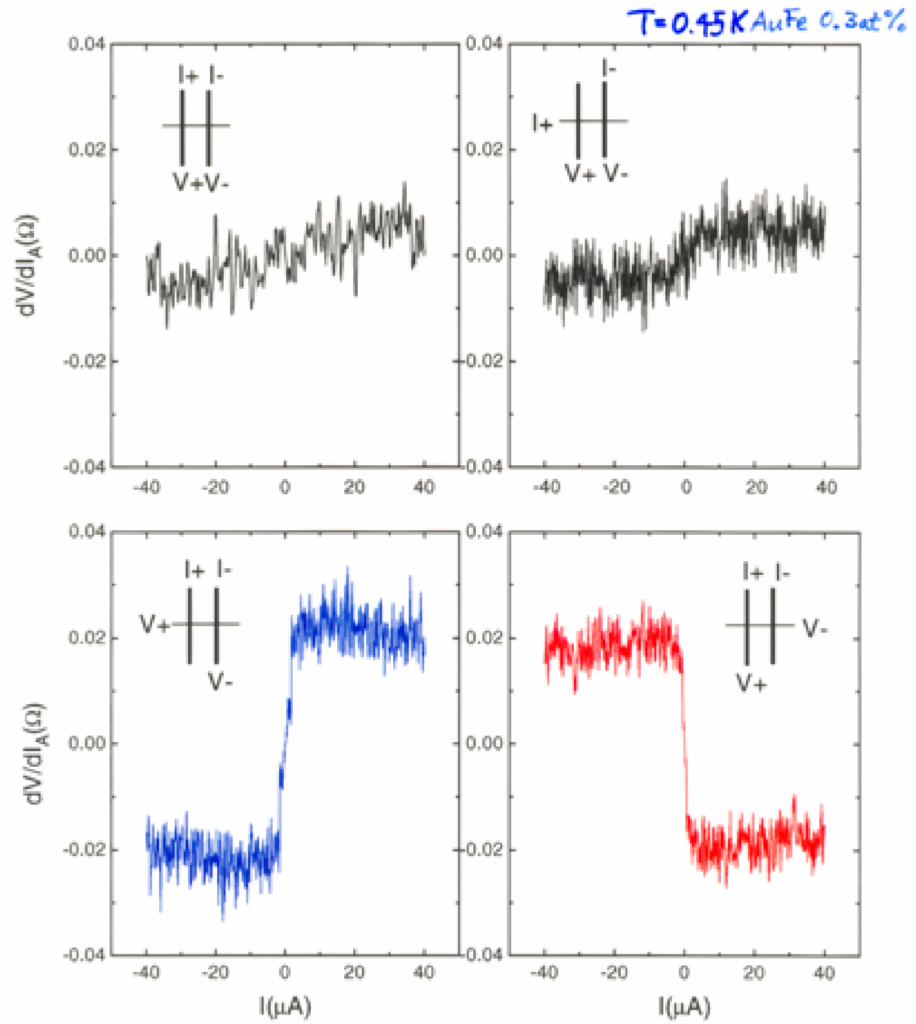

Voltage probe의 width가 서로 다를 때 dV/dI는 asymmetric하게 나온다.

Temperature dependence of antisymmetric part of dV/dI

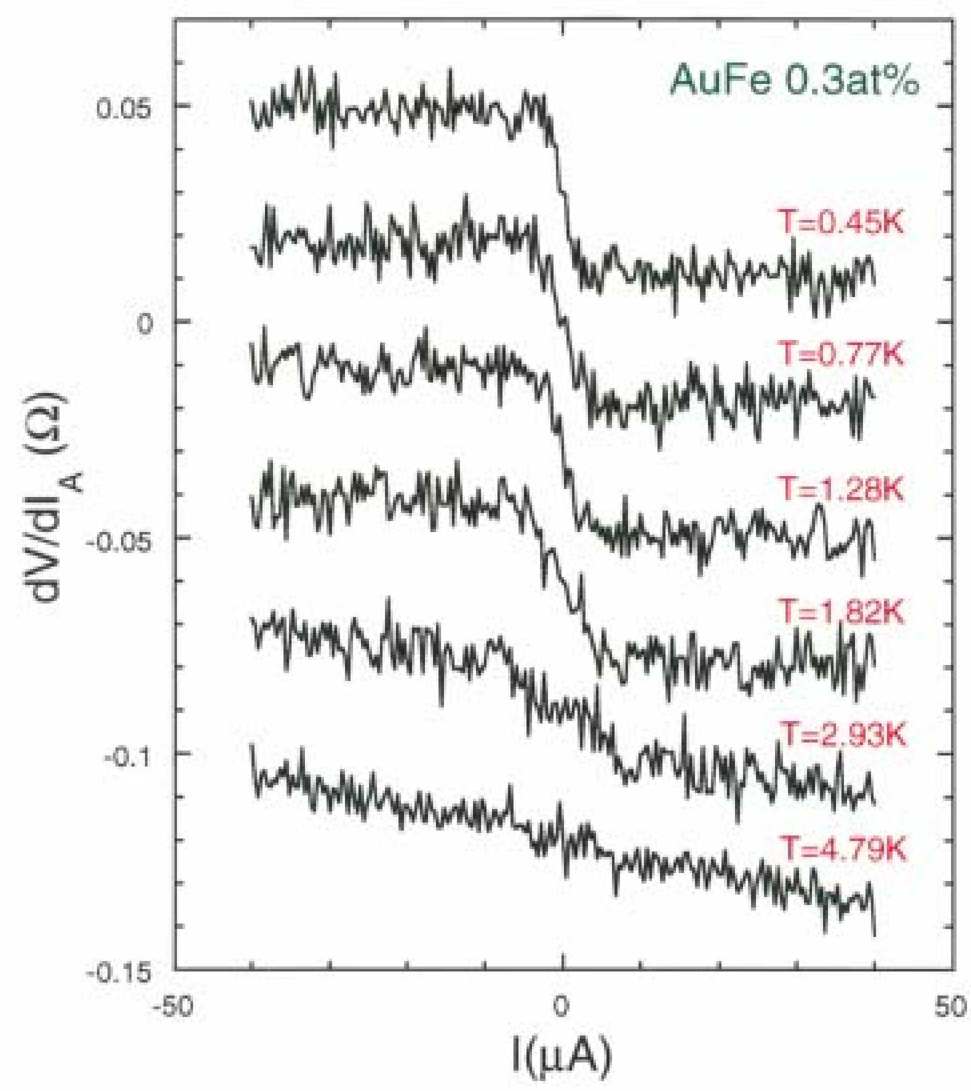

Thermoelectric effect

Measurement configuration

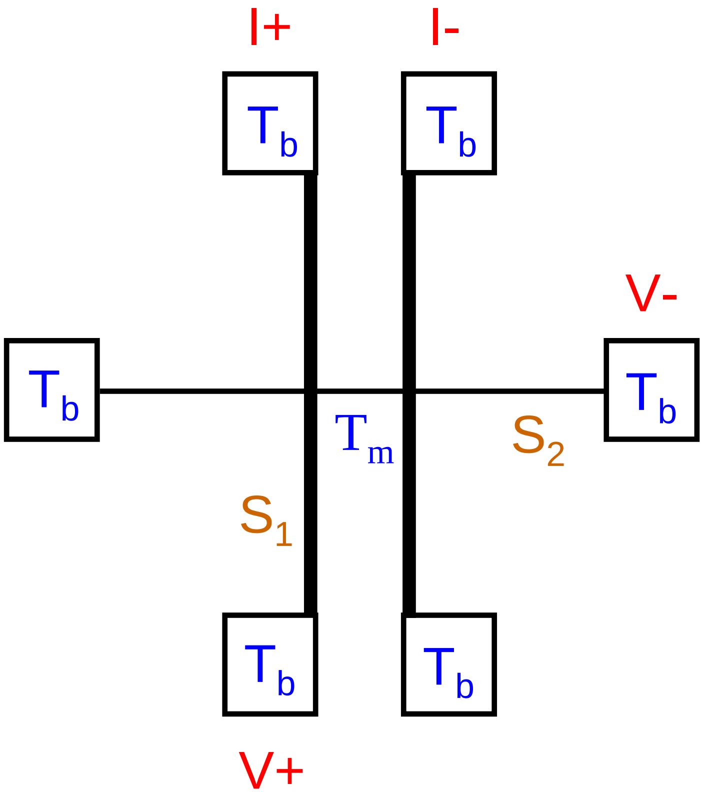

Measured voltage

$$V = I\,R + \int_{T_b}^{T_m(I)} S_1\,dT + \int_{T_m(I)}^{T_b} S_2\,dT$$

$$= I\,R + \int_{T_b}^{T_m(I)} (S_1 - S_2)\,dT$$

where S_1 : thermopower of wide wire

S_2 : thermopower of narrow wire

$$\boxed{\frac{dV}{dI} = R + [S_1 - S_2]_{T=T_m} \times \frac{dT_m}{dI}}$$

Resistance
(symmetric in I)

thermoelectric part
(antisymmetric in I)

T_m(I) 을 구하면 dV/dI 측정값으로부터 wire의 width에 따른 ΔS 를 알 수 있다.

Electron heating by dc current

K.E. Nagaev, PRB 52, 4740 (1995)

$$\frac{\pi^2}{3} k_B{}^2 L^2 \frac{\partial}{\partial x}\left(T_e \frac{\partial\, T_e}{\partial\, x}\right) = -(eIR)^2 + \frac{24\zeta(5)\alpha_{ph} L^2 k_B{}^5}{(k_B \Theta_D)^2 \hbar D}(T_e{}^5 - T_b{}^5)$$

Electronic heat conduction through wire itself

Joule heating

electron-phonon coupling

$T_m(I)$ can be obtained for each bath temperature T_b

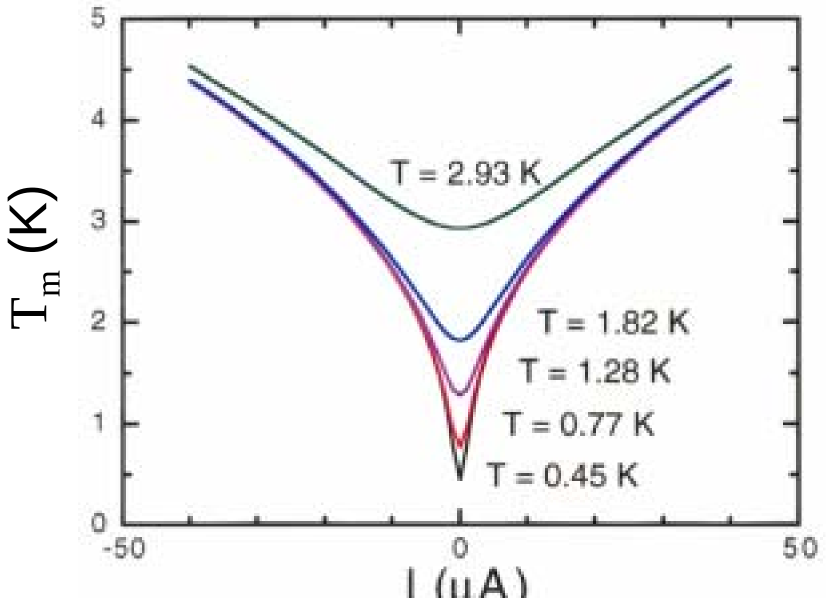

ΔS (= $S_{110nm} - S_{60nm}$) 의 온도의존성

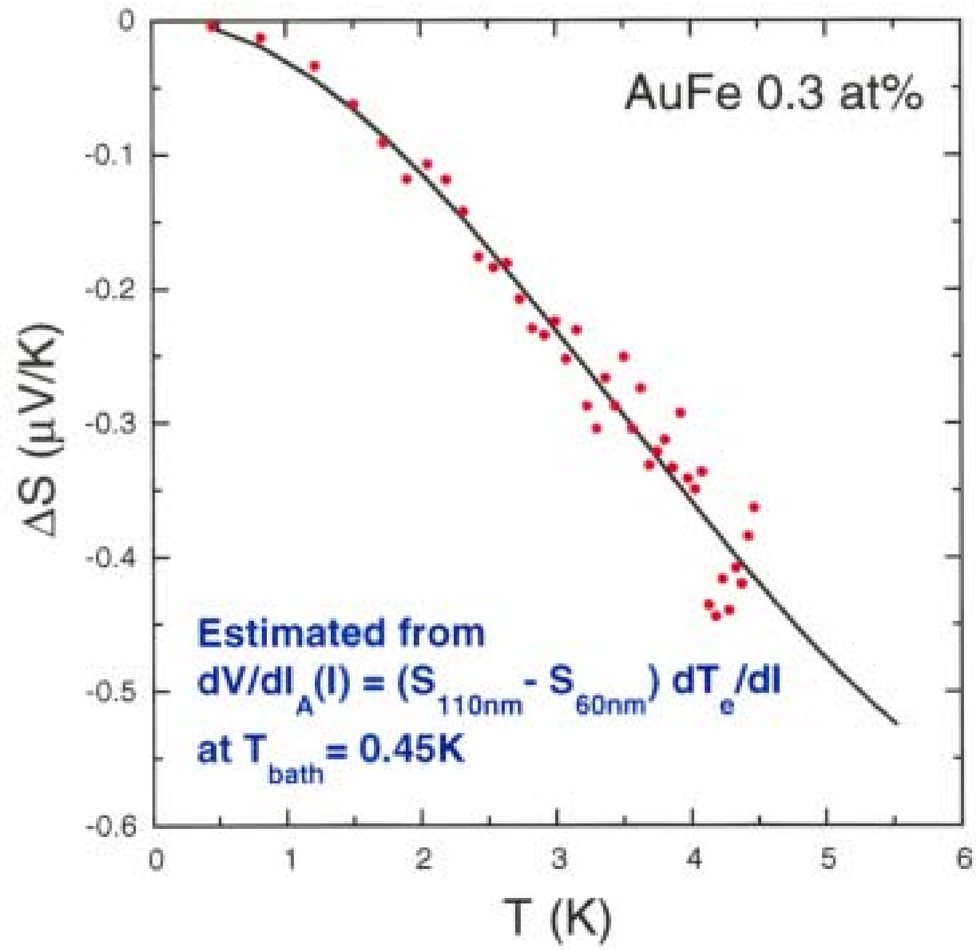

AuFe spinglass의 thermopower는 size effect 가 있다.

Size dependent thermopower in Mesoscopic AuFe wires

AuFe(0.3%) film thickness = 30 nm

Strunk et al., PRL 81, 2982 (1998)

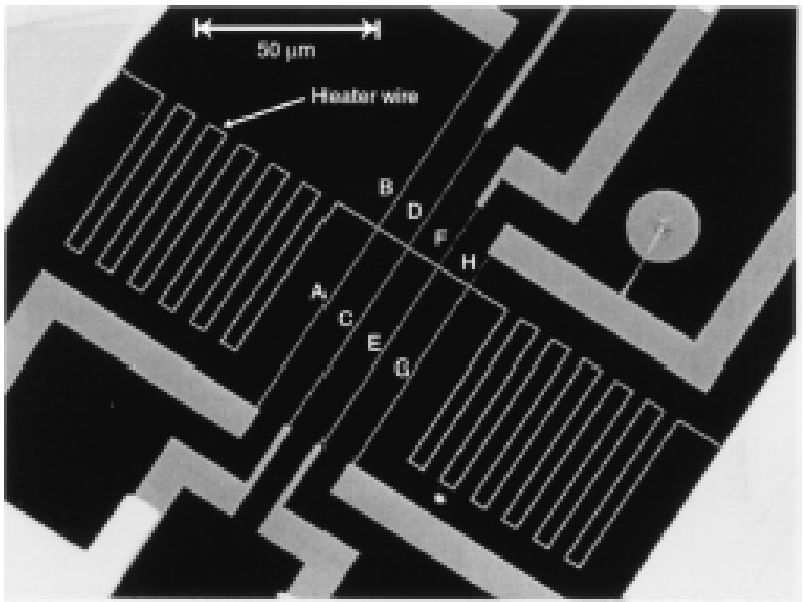

Antisymmetric part of dV/dI

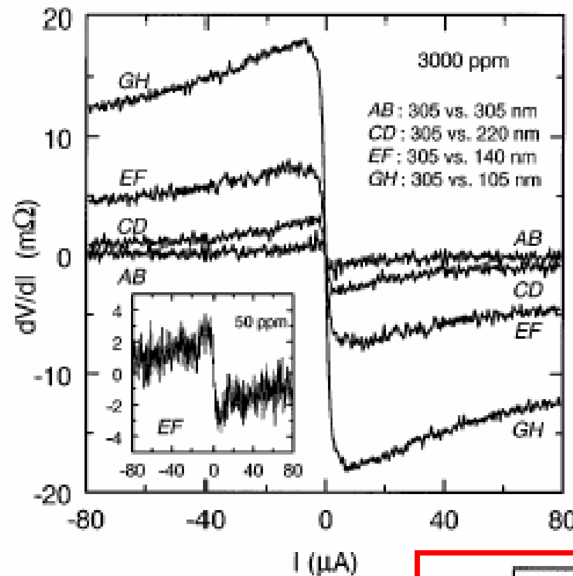

Measuring T_m by noise spectrum

; Henny et al., APL 71, 773 (1997)

$$S_V(I) = 4kT_m(I)R$$

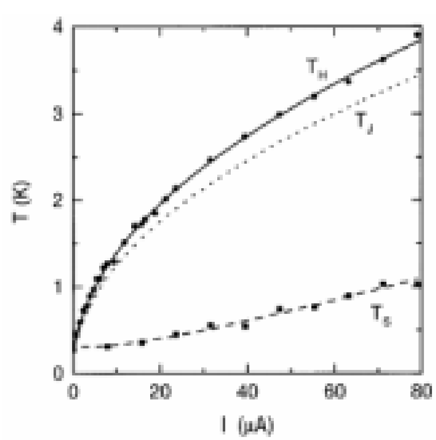

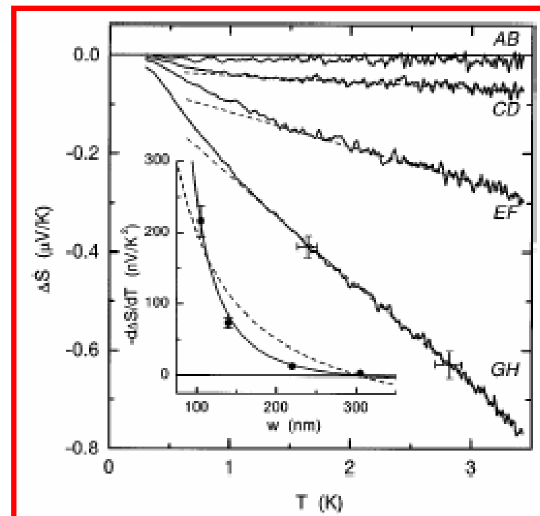

Superconducting proximity effect in Kondo alloys

Eom, JKPS 42, L313 (2003)

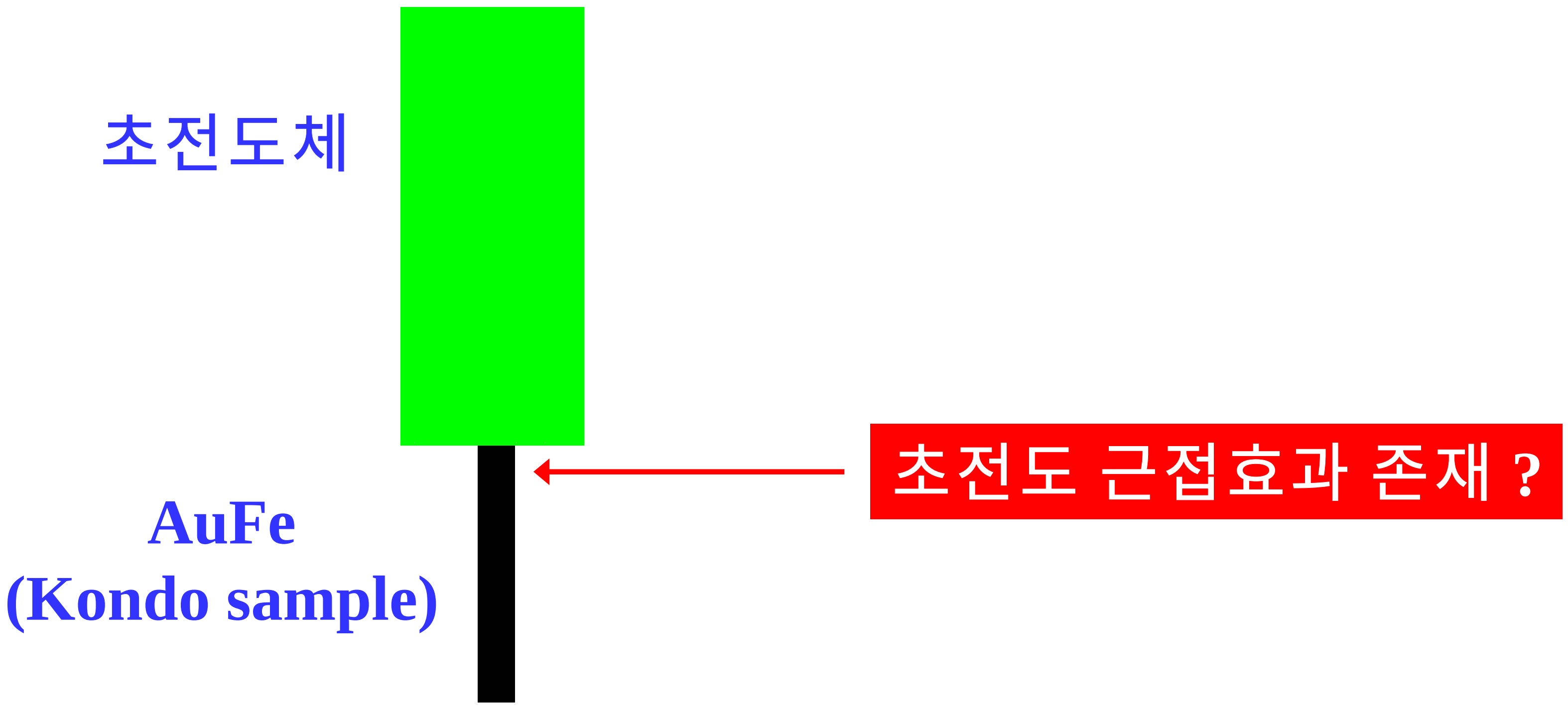

Magnetic impurity에 의해 phase coherence length (L_φ)가 매우 짧아진 경우, 과연 초전도 근접효과**(**장거리 효과**)**가 존재할까**?**

Motivation

강자성체내에서의 초전도 근접효과?

강자성체내의 **exchange field =>** $\xi_{ex} = \sqrt{\dfrac{hD}{2\pi k_B T_{Curie}}} \approx$ **1-3 nm**

: 초전도근접효과는 **transport** 특성에 큰 영향을 미치지 않으리라 예견

(Kawaguchi et al., PRB 1992의 실험: Fe/Nb multilayer)

근래 mesoscopic F/S structures에 대한 실험들

1. **Superconducting proximity effect in a mesoscopic ferromagnetic wire**
   ; Giroud et al., PRB (1998).
2. **Proximity effects in superconductor-ferromagnet junctions**
   ; Lawrence and Giordano, J. Phys. (1999).
3. **Giant mutual proxomity effects in F/S nanostructures**
   ; Petrashov et al., PRL (1999).

=> ξ_{ex} 보다 훨씬 먼 영역까지 초전도 영향

기본적인 물리현상 : Andreev 반사

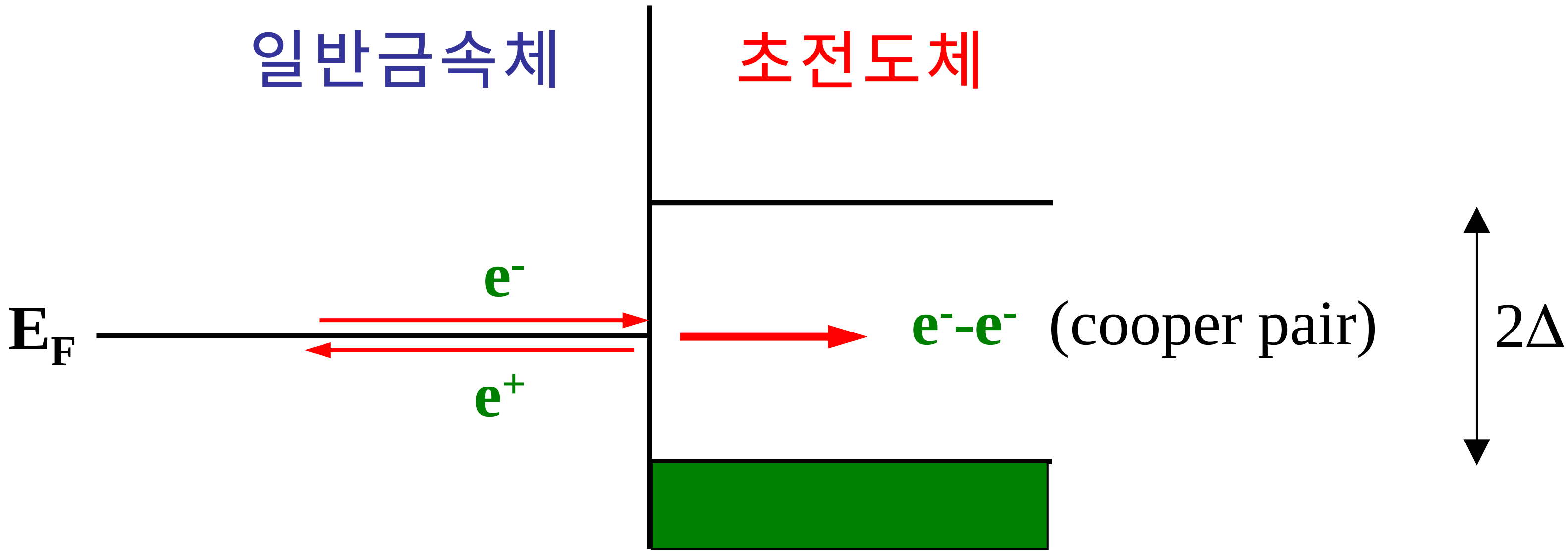

1. 초전도체 갭 에너지보다 낮은 값을 가지는 전자는 초전도체로 진행 못 한다.
2. 그러나, 안드레프 반사를 하면서 **cooper pair**를 만들면 전자의 진행이 가능.

안드레프 반사의 중요 특성 :

(a) 전자의 위상값이 초전도의 위상값으로 전달 (Phase-memory effect).
(b) 정공은 전자의 행로를 따라 되돌아 간다 (Retro-reflection).

N/S에서 초전도 근접효과 (장거리 효과)

비자성체/초전도체 (N/S) 접합 구조물

- 초전도 pair correlation은 비자성 금속체속으로
  L_T ($= (hD/2\pi kT)^{0.5}$) 만큼 스며들어간다.
- Au 박막의 경우 L_T 는 온도 1 K 에서 ~ 0.3 μm 정도이다.

참고서적: Hekking, Schoen, Averin, ***Mesoscopic Superconductivity***
Physica (Amsterdam) 203B (1994).

AuFe 나노선/Al 박막 혼합구조

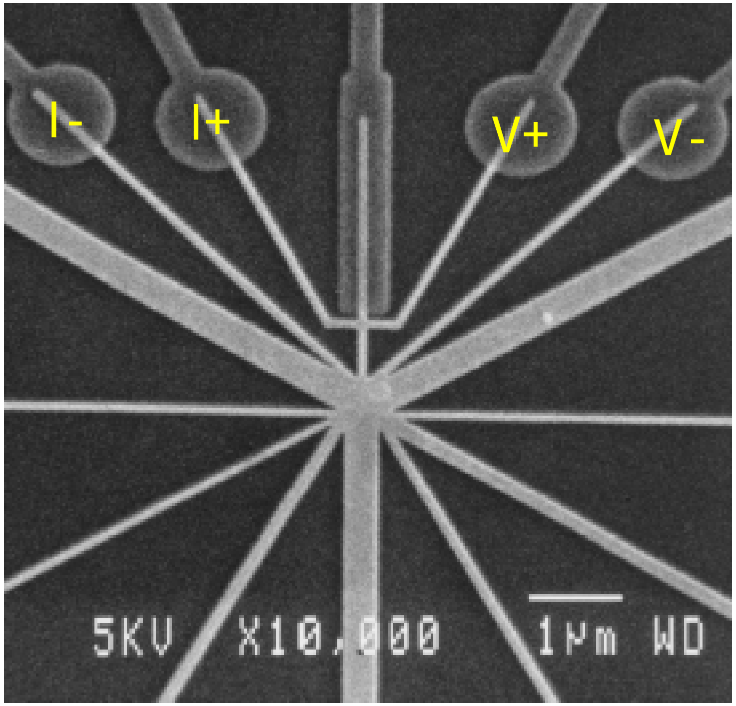

Kondo sample

Fe 농도 : 100 ppm (0.01%)

Film 두께
AuFe = 51 nm
Al = 75 nm (T_C = 1.15 K)

측정되는 부분은 AuFe/초전도 접합을 포함하지 않는다.

온도 특성

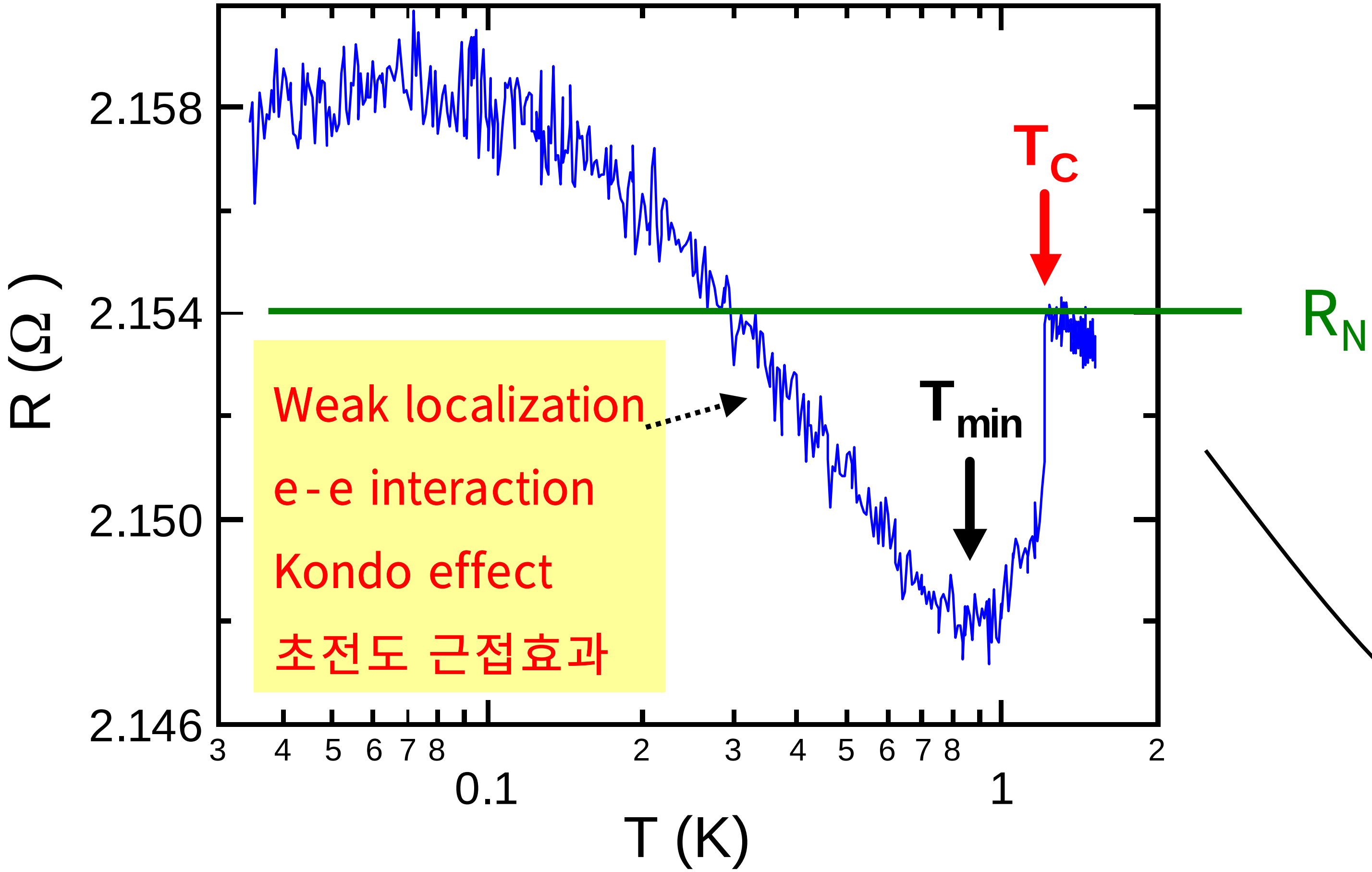

2.158
2.154
2.150
2.146
R (Ω)
3 4 5 6 7 8 0.1 2 3 4 5 6 7 8 1 2
T (K)
T_C
R_N
T_{min}
Weak localization
e-e interaction
Kondo effect
초전도 근접효과

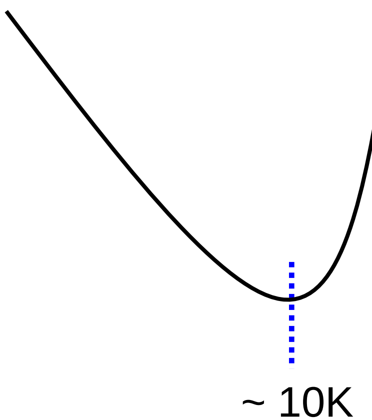

~ 10K

Repulsive e-e interaction correction

Altshuler and Aronov (1985)

$$\delta\rho_{ee}(T) - \delta\rho_{ee}(T_0) = \alpha \frac{R_{\square}^2 t}{(\pi\hbar / e^2)W} L_T$$

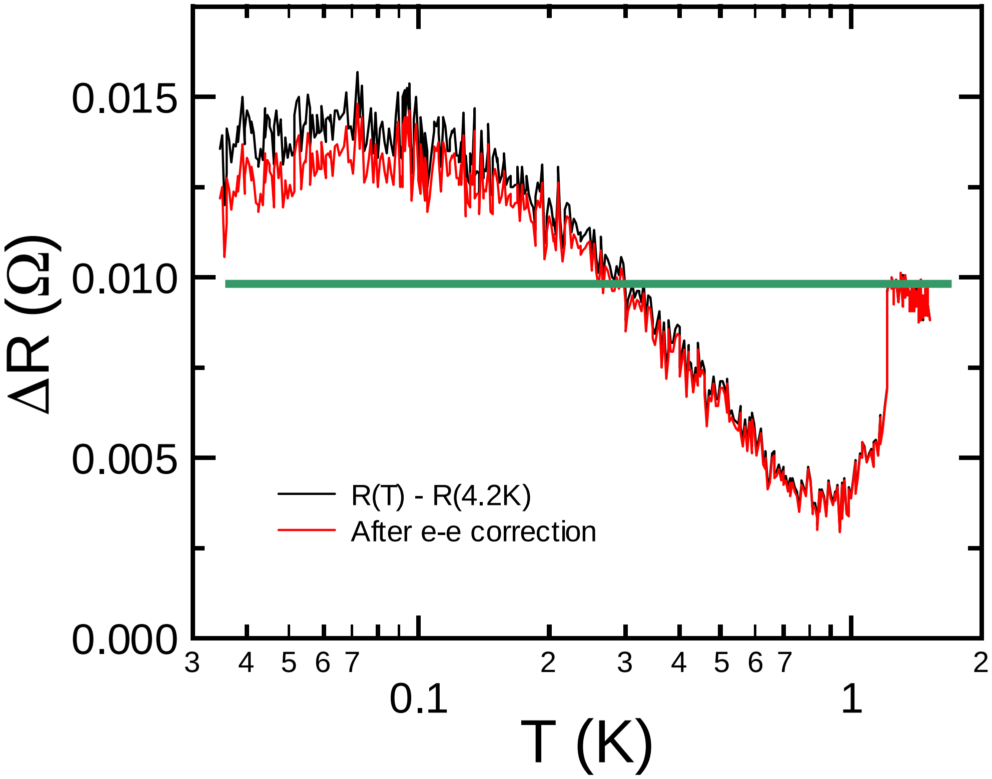

e-e interaction 에 의한
저항 보정값은 미미하다.

Temperature dependence of Kondo resistivity

When $T \ll T_K$, $\rho \sim \rho_0 - cT^2$

$T_K \ll T$ 일 때, $\Delta\rho(T) \propto \ln(T / T_K)$

$T \sim T_K$ 일 때, Hamann expression (Phys. Rev. 1967)

$$\Delta\rho(T) \propto \frac{1}{2}\rho_0\left(1 \pm \left[1 + \frac{S(S+1)\pi^2}{[\ln(T / T_K)]^2}\right]^{-\frac{1}{2}}\right)$$

$T_K > T$ 일 때, 수식에서 (-) 부호,
$T_K < T$ 일 때, 수식에서 (+) 부호를 취한다.
여기서, ρ_0 는 자성물질의 농도에 비례한다.

$\Delta\rho$ 를 fitting 해서 T_K와 S를 구할 수 있다.

Fitting by Hamann expression

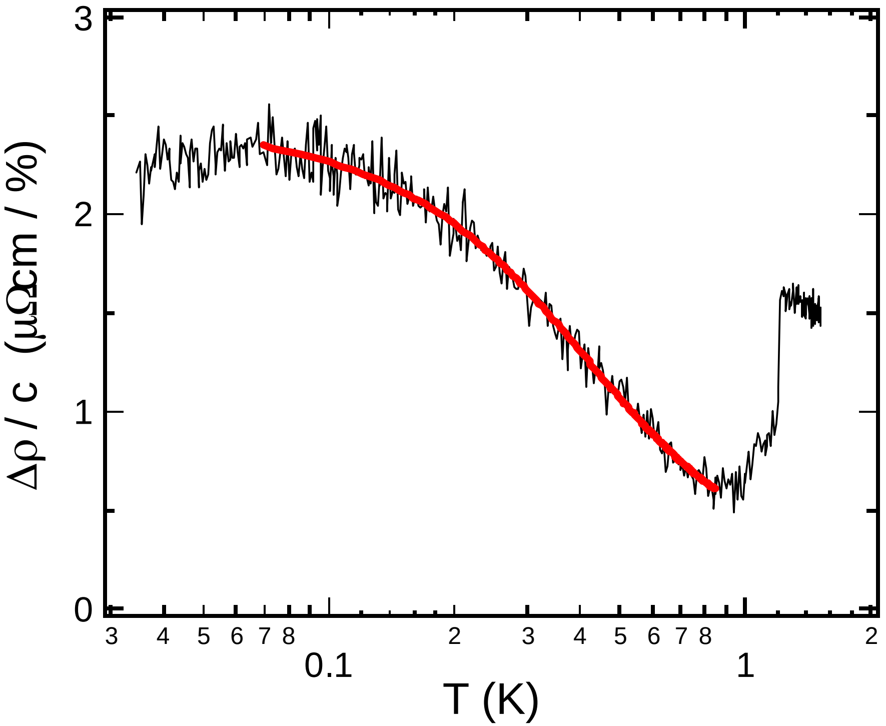

Fit parameter : T_K = 0.41 K, S = 0.12

T_K 는 초전도영향권에 있지 않은 AuFe의 T_K와 비슷하다.
그러나 S 는 (0.5~1.0) 사이가 아니다.

=> 초전도의 영향때문에 Kondo 현상이 수정되었다.

AuFe 나노선/Al 박막 혼합구조

Fe 농도 : 100 ppm (0.01%)

Al = 75 nm
AuFe = 51 nm

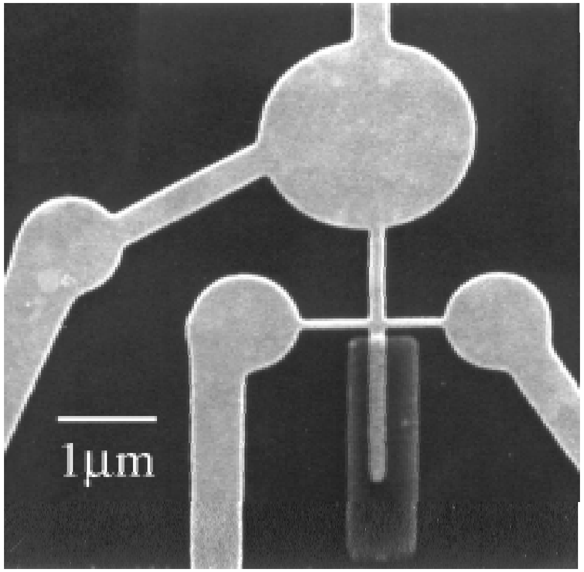

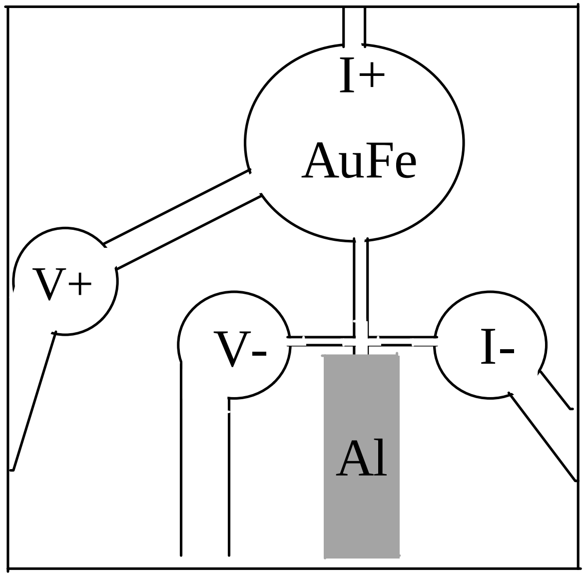

측정되는 부분은 AuFe/초전도 접합을 포함하지 않는다.

Fitting by Hamann expression

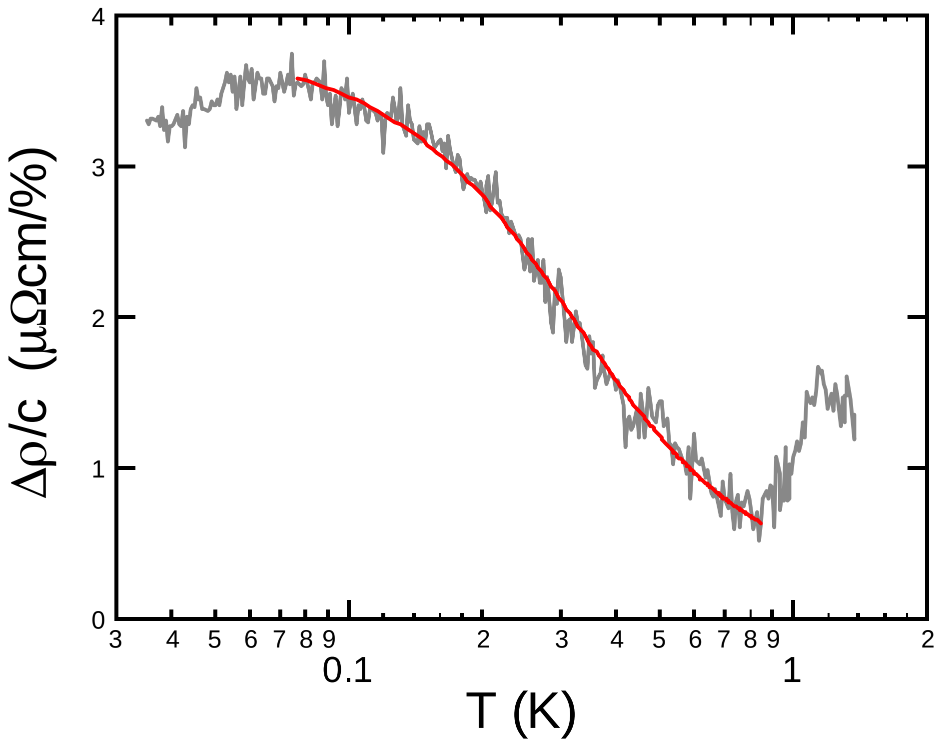

Fit parameter : T_K = 0.32 K, S = 0.10

T_K 는 일반적인 **AuFe**의 T_K와 비슷하다.
그러나 S 는 0.5~1.0 사이가 아니다.

=> 근접효과에 의해서 Kondo 현상이 수정되었다.

Mesoscopic dilute magnetic systems

- Kondo regime

Kondo length for a typical AuFe films:

$$\xi_K = \frac{hv_F}{k_B T_K} \approx 20\mu m$$ **in ballistic limit**

$$\xi_K = \sqrt{\frac{hD}{k_B T_K}} \approx 0.5\mu m$$ **in diffusive limit**

현재 **lithography** 기술로 충분히 도달할 수 있는 길이이며, 실험으로써 연구 가능한 영역이다.

II. Kondo effect in low- dimensional systems

Kondo effect in a single electron transistor

Kondo effect in carbon nanotubes

Kondo effect in a single molecule transistor

Kondo effect in a single electron transistor

MIT and Weizman Institute of Science

- Kondo effect in a SET; Nature 39, 156 (1998).
- From the Kondo regime to the mixed-valence regime in a SET ; PRL 81, 5225 (1998)

Delft University, Netherlands

- A tunable Kondo effect in quantum dots; Science 281, 540 (1998)
- The Kondo effect in the unitary limit; Science 289, 2105 (2000)
- Kondo effect in an integer-spin quantum dot; Nature 405, 764 (2000)

Ludwig-Maximilians-Universitat, Germany

- Anomalous Kondo effect in a QD at nonzero bias; PRL 83, 804 (1999)

Max-Planck-Institute, Germany

- Quantum dot in high magnetic fields; PRB 64, 033302 (2001)

Cavendish Laboratory, UK

- Kondo effect in a quantum antidot; PRL 89, 226803 (2002)

Example of sample structures of 2DEG

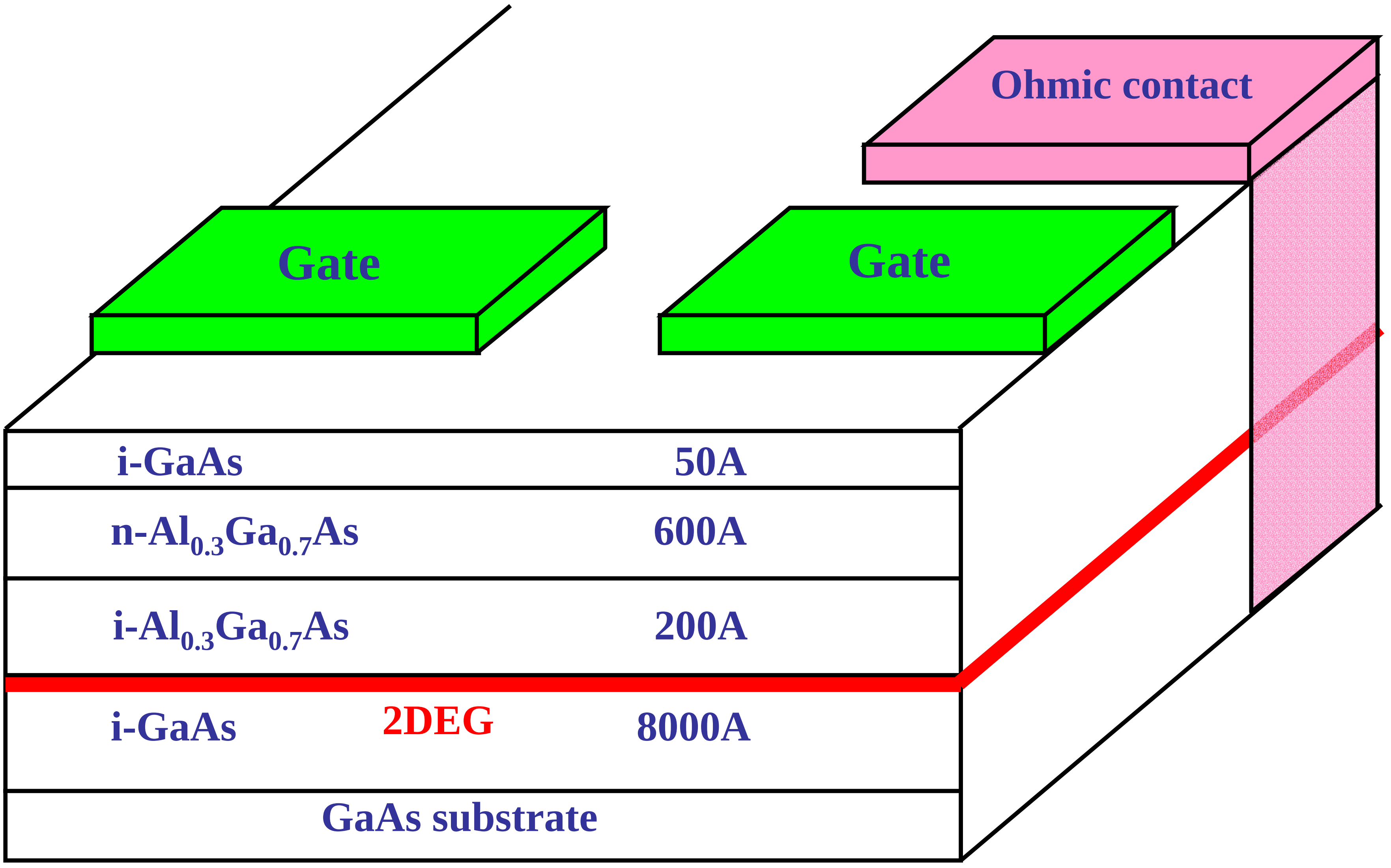

Coulomb blockade oscillation

When $kT < e^2/2C$

Kastner, Phys. Today 24 (Jan 1993)

Electrostatic energy of a charge Q on the dot

$$E = QV_g + \frac{Q^2}{2C} = \frac{1}{2C}(Q + CV_g)^2 - CV_g^2$$

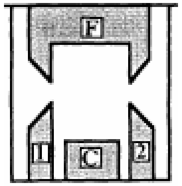

gate

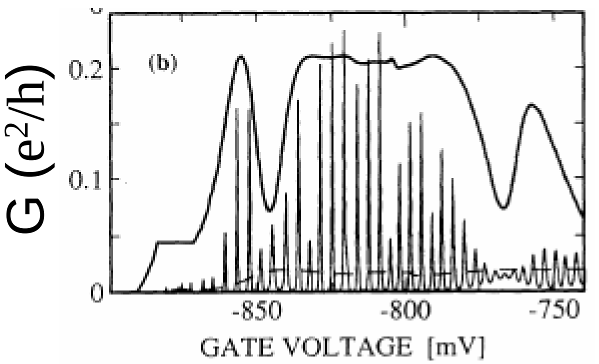

Johnson et al., PRL 69, 1592 (1992)

$Q = \ldots, -(N+1)e, -Ne, -(N-1)e, \ldots$

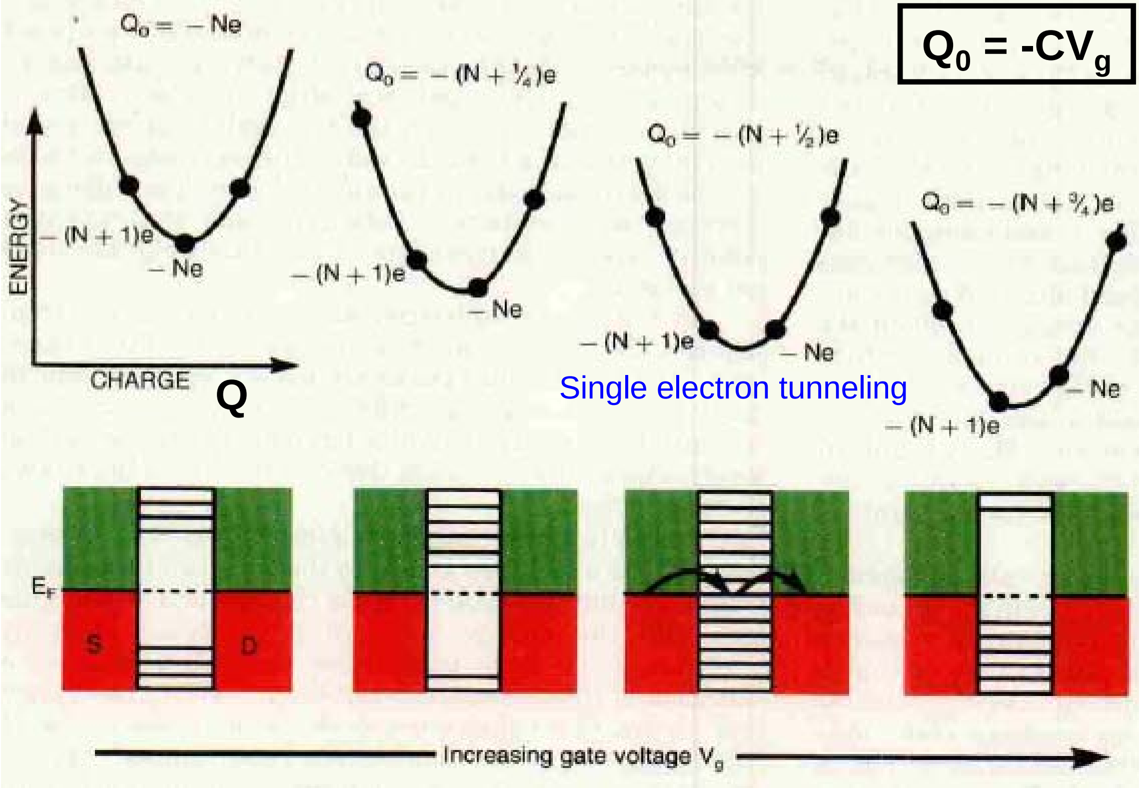

Evenly spaced oscillation

$\Delta V_g = e/C$

Co-tunneling (2^{nd} order process)

Glazman and Pustilnik, cond-mat/0302159

At low temperatures, $T \ll E_C$, conduction through the dot in the Coulomb blockade valleys is exponentially suppressed.

Going beyond the lowest-order perturbation, the following "co-tunneling" process contributes to the activationless transport.

Inelastic co-tunneling

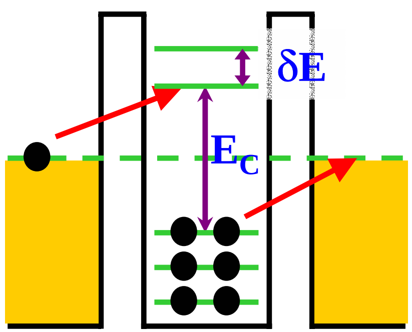

$$G_{in} \propto \frac{e^2}{h} G_L G_R \left(\frac{T}{E_C} \right)^2$$

e-h pair를 남긴다.

Elastic co-tunneling

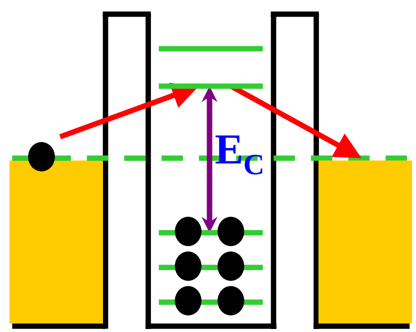

Non spin-flip

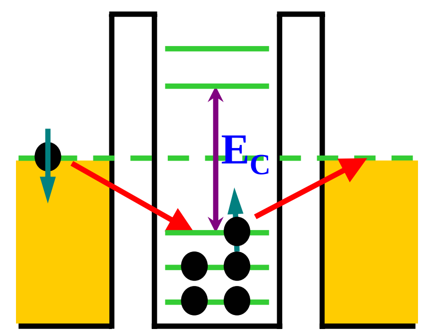

Spin-flip

Transmission amplitude diverges logarithmically when the energy of an incoming electron approaches 0.

T dependence of the conductance in the Coulomb blockade valley with N_d= odd

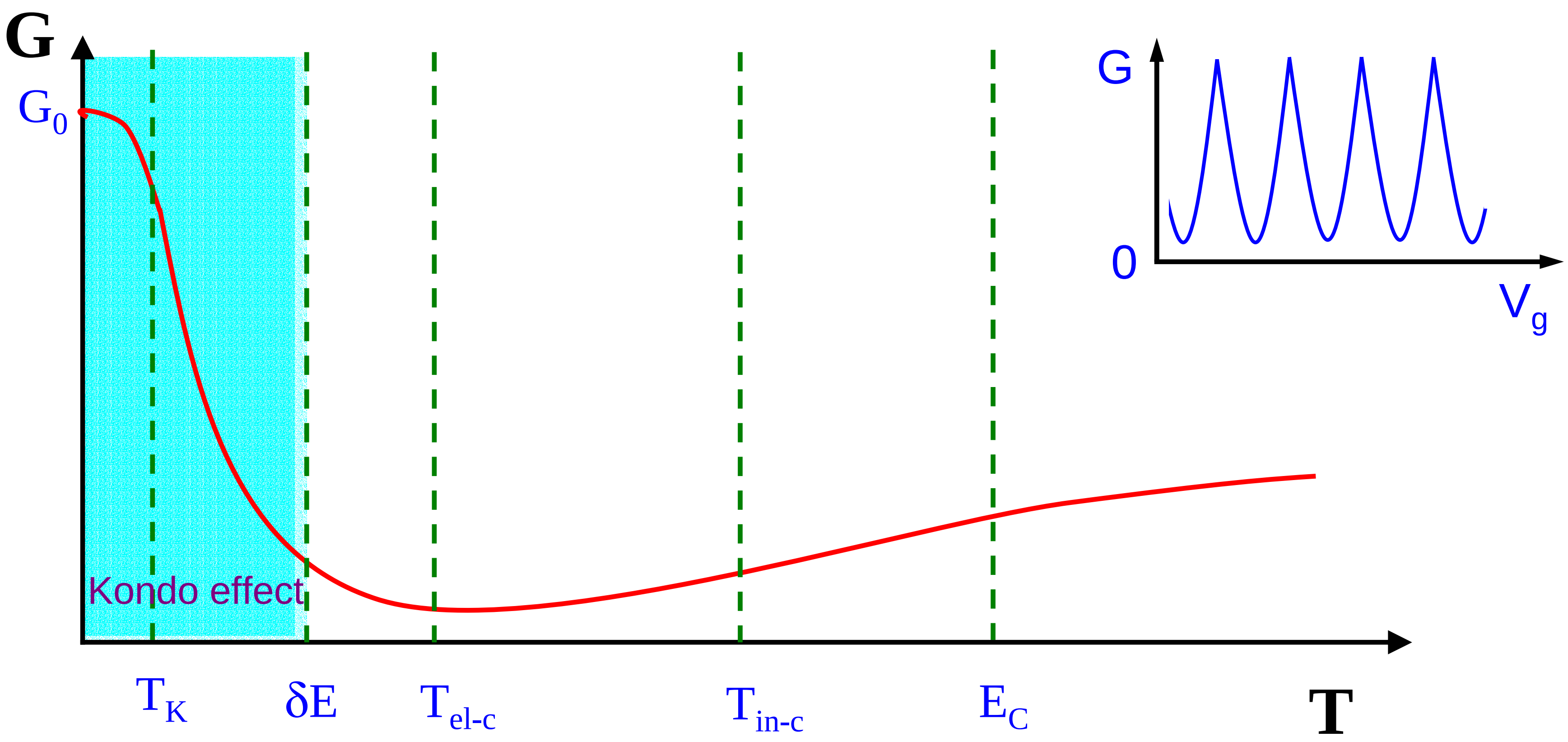

$$G = G_0 \,[1 - (\pi T / T)^2] \quad \textit{where} \quad T \ll T_K$$

$$G = G_0 \frac{3\pi^2/16}{[\ln(T/T_K)]^2} \quad \textit{where} \quad T_K \ll T \ll \delta E$$

Single electron transistor (SET)

SET is approximated as a single localized state (Anderson model).
Electron tunnels into the leads with rate Γ/h.

Kondo temperature : $k\,T_K \approx 4 - 250\mu eV \qquad (T_K \approx 0.05 - 3\ K)$

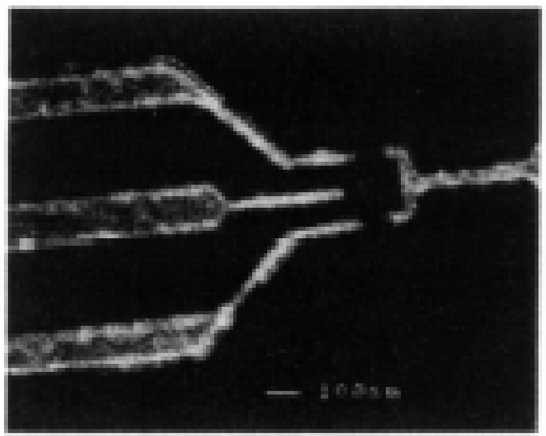

Goldhaber-Gordon et al., PRL 81, 5225 (1998)

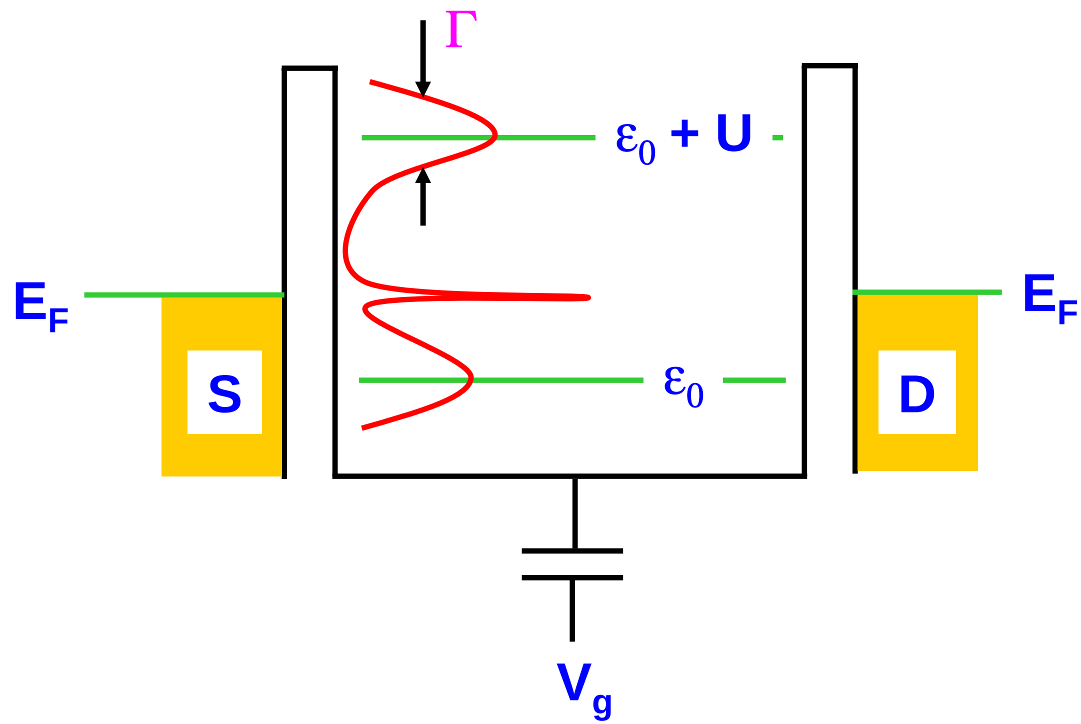

where

ε_0 : bare-level energy

U : Coulomb interaction energy

Advantages of quantum dot in 2DEG

1. Tunneling rate of leads (Γ) is controlled by the point-contact Voltage.

ε_0 / Γ << - 0.5 : Kondo regime

- 0.5 < ε_0 / Γ < 0 : mixed-valence regime

ε_0 / Γ > 0 : empty orbital regime

2. ε_0 of quantum dot is controlled by V_g

$\varepsilon_0 = \alpha e V_g$ + const.

α **:** coupling constant to relate V_g and ε_0.

3. Γ 와 α 는 실험결과로부터 구해 낼 수 있다.

Constant interaction model

Charging energy U is assumed to be constant, independent of the number of electrons in quantum dot.

Conductance of resonant tunneling at T = 0

$$G_{T=0} = 2\frac{e^2}{h}\frac{\Gamma_L\Gamma_R}{(E-E_0)^2+\Gamma^2}$$

where $\Gamma = (\Gamma_L + \Gamma_R)/2$

at finite T

$$G = 2\frac{e^2}{h}\frac{\Gamma_L\Gamma_R}{4\Gamma^2}\int dE\left\{\frac{\Gamma_L\Gamma_R}{(E-E_0)^2+\Gamma^2}\right\}\left(-\frac{df}{dE}\right)$$

$$= 2\frac{e^2}{h}\frac{\Gamma_L\Gamma_R}{\Gamma^2}\int\frac{dE}{kT}\left\{\frac{\Gamma_L\Gamma_R}{(E-E_0)^2+\Gamma^2}\right\}\operatorname{sech}^2\left(\frac{E-\alpha eV_g}{2kT}\right)$$

FWHM of G is given by $\Delta = \dfrac{0.78\Gamma + 3.52kT}{\alpha\, e}$

Obtaining α and Γ from experiment

Goldhaber-Gordon et al., PRL 81, 5225 (1998)

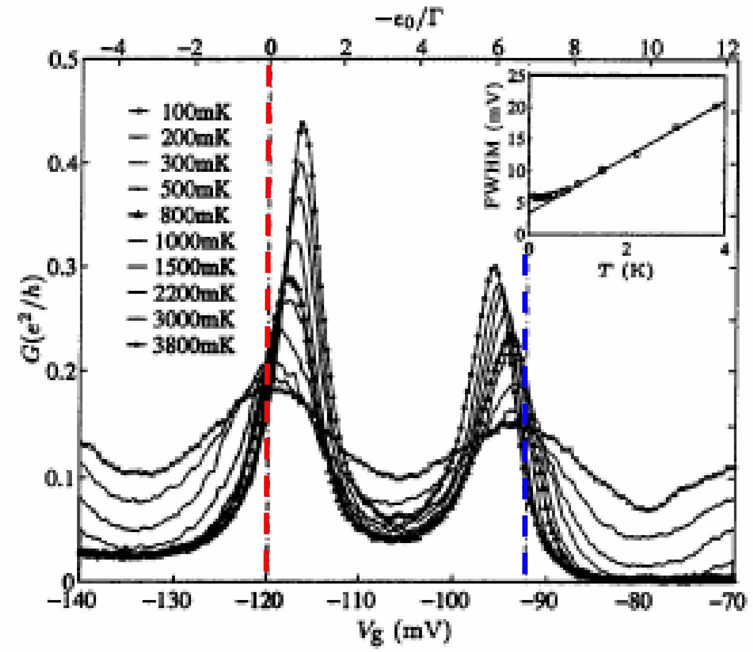

n_d = 0 1 2

FWHM of the left peak

$$\Delta = \frac{0.78\Gamma + 3.52kT}{\alpha e}$$

Fitting에 의해 α 와 Γ 를 구할 수 있다.

α = 0.069 ; Γ = 295 μeV

Coulomb interaction energy

$U = \alpha e \Delta V_g = 1.9$ meV

Recall

$\varepsilon_0 = \alpha e V_g + \text{const.}$

Kondo effect in a single electron transistor

van der Wiel et al., Science 289, 2105 (2000)

T=15 mK

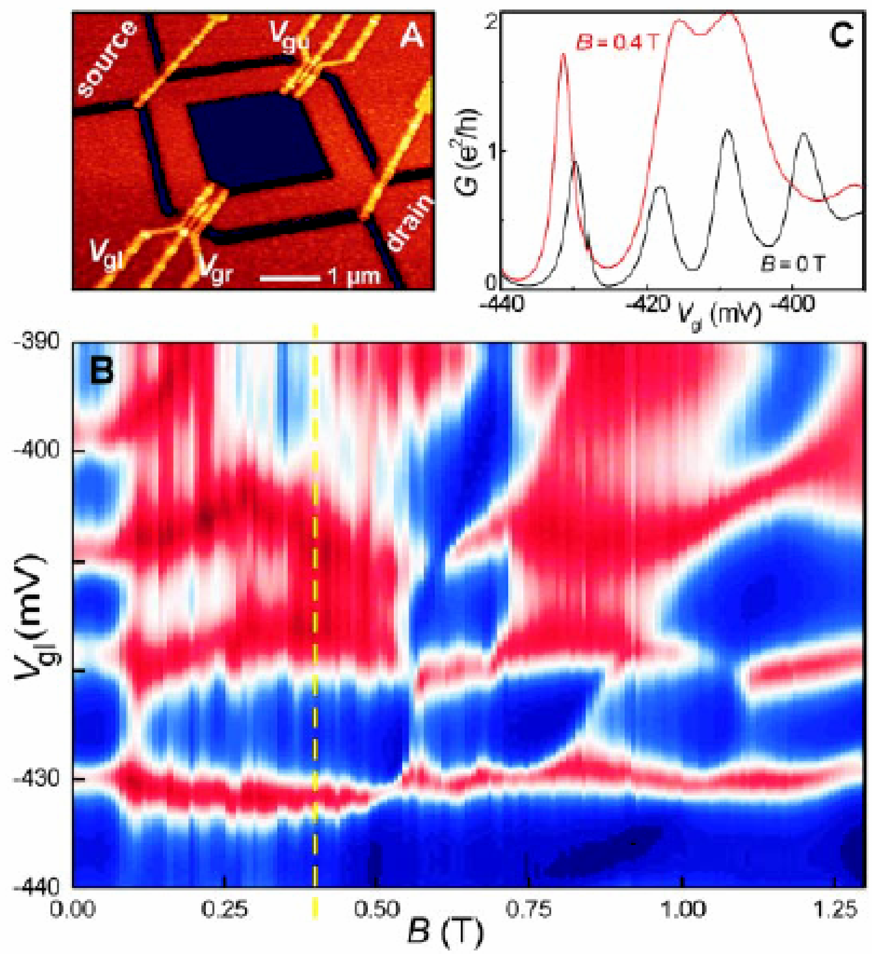

- Upper gate (V_{gu}) pinches off the upper arm.
- Regular Coulomb blockade oscillations at B=0.
- Small B brings about a different transport regime (stronger Kondo effect).

Unitary limit of the Kondo effect in SET

온도대역: 15 mK – 800 mK,   B= 0.4T

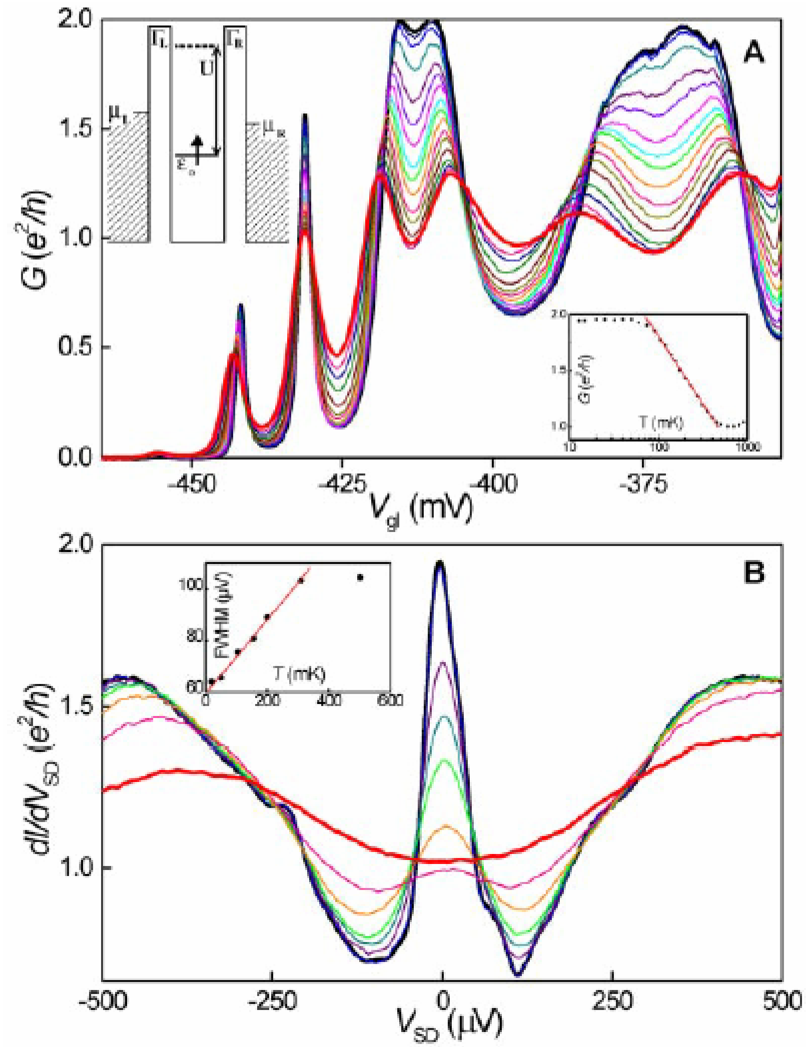

G(T)

G at V_{gl} = -413mV shows
logarithmic T dependence (inset),
and saturates below 90mK (unitary limit)

This experiment shows a unitary limit
= $2e^2/h$ ($\Gamma_R=\Gamma_L$의 경우)

Kondo resonance peak

V_{gl} was fixed at -413mV.
V_{SD} was biased between S and D.

Kondo temperature: T_K

T_K in Log scale

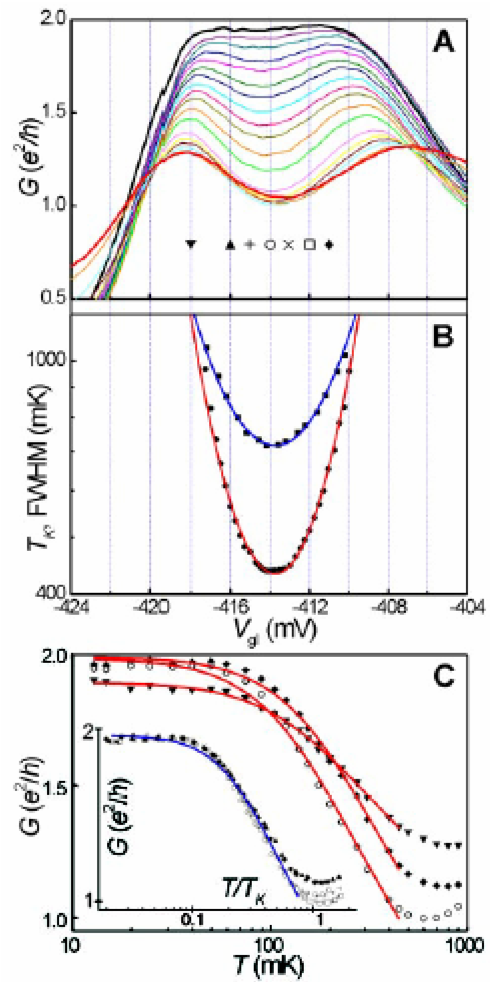

In Anderson model,

; Costi et al., J. Phys.: Condense. Matter **6**, 2519 (1994)

$$kT_K = \frac{\sqrt{\Gamma U}}{2} \exp\left[\frac{\pi\varepsilon_0(\varepsilon_0 + U)}{\Gamma U}\right]$$

An empirical function

; Goldhaber-Gordon et al., PRL **81**, 5225 (1998)

$$G(T) = G_0 \left(\frac{1}{1 + (2^{1/S} - 1)\ T^2 / T_K^2} \right)^S$$

: universal functional form of T/T_K

- T_K is obtained from fitting.
- S is a fit parameter, but is almost constant (~ 0.2) in the Kondo regime.

AB conductance oscillation and Coulmob blockade oscillation

conductance maximum

Aharonov-Bohm oscillation

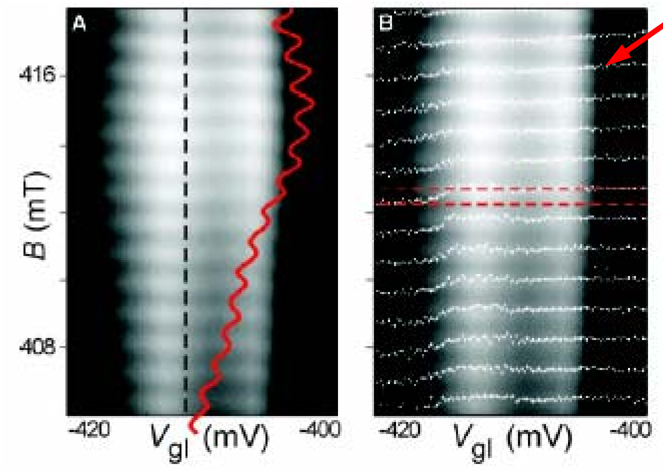

Coulomb blockade oscillation

π–phase flip is observed when stepping through the left Coulomb peak

2-treminal geometry causes rapid phase change by π.

; Yacoby et al., PRB 53, 9583 (1996)

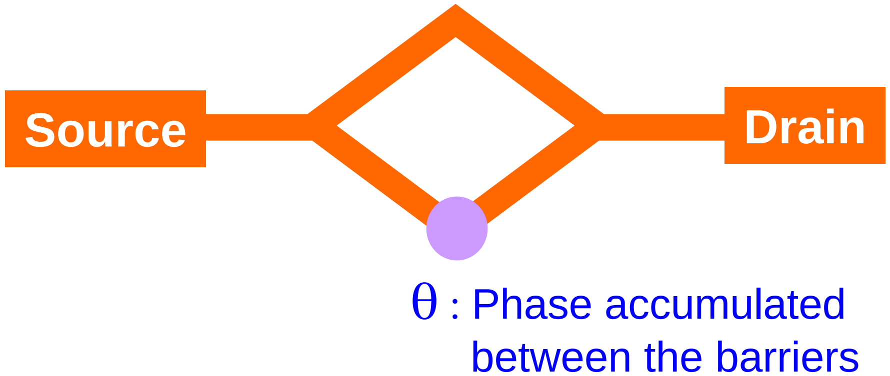

No phase change is observed in right Coulomb peak.

Why? Yet to be understood.

Kondo effects in carbon nanotubes

Nygard et al., Nature 408, 342 (2000)

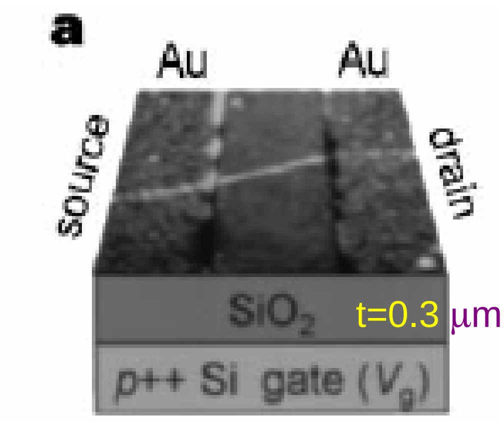

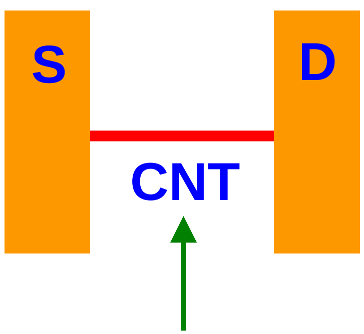

1-D quantum dots
(Kondo impurity)

Carbon Nanotube

L=300 nm, 2 nm dia.
metallic single-walled carbon nanotube

Au contact과 CNT사이의 transmission probability P

P << 1 : Coulomb blockade
P ~ 0.9 : diffusive 1-D wire
intermediate P : Kondo effect

Kondo resonances for many quantum dots

The number of quantum dots is about number of carbon atoms : ~ 수 만개

Various structures of carbon nanotube

http://home.hanyang.ac.kr/~nanotube

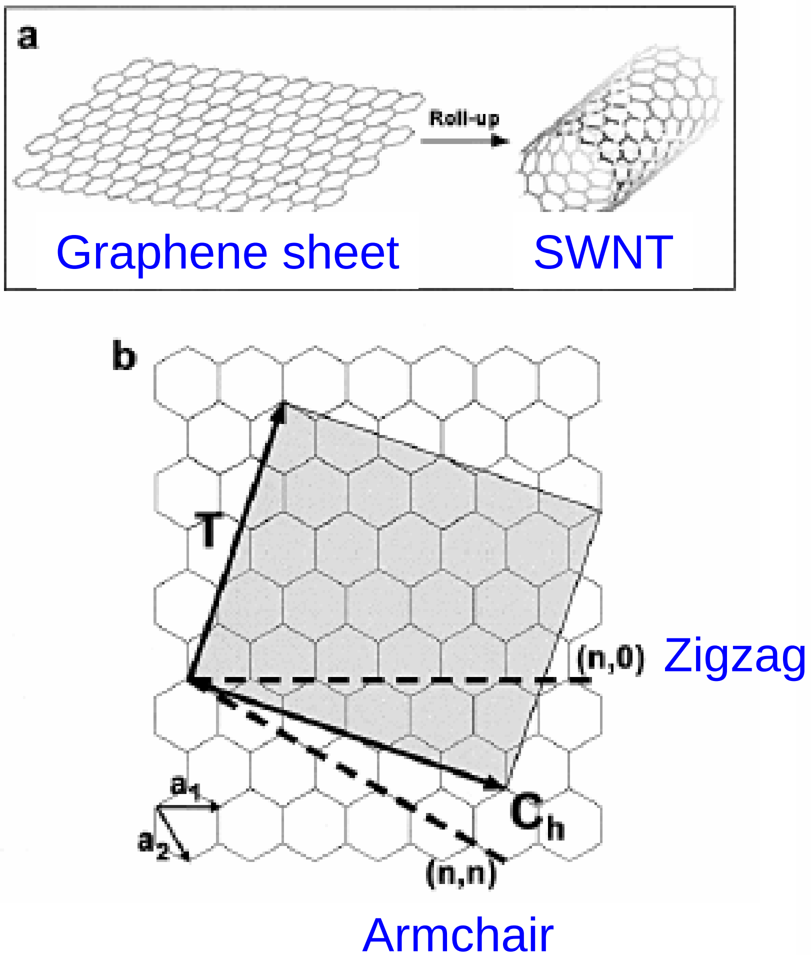

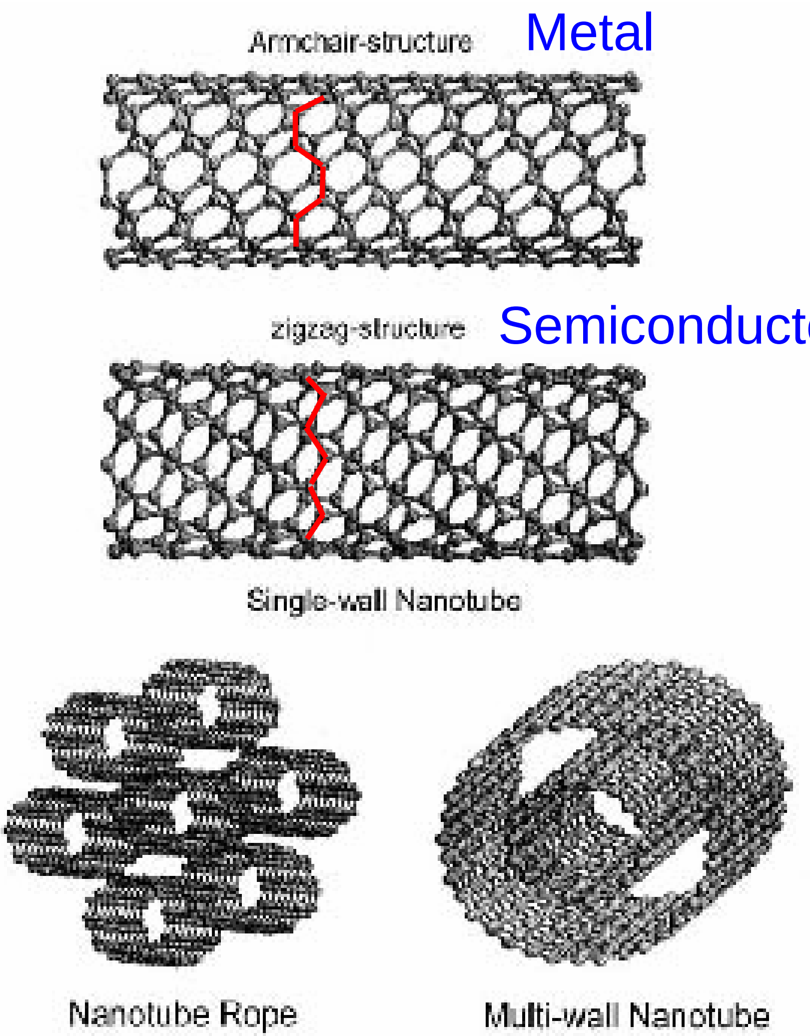

Fig. 1. Various structures of carbon nanotubes.

Temperature dependence of conductance G

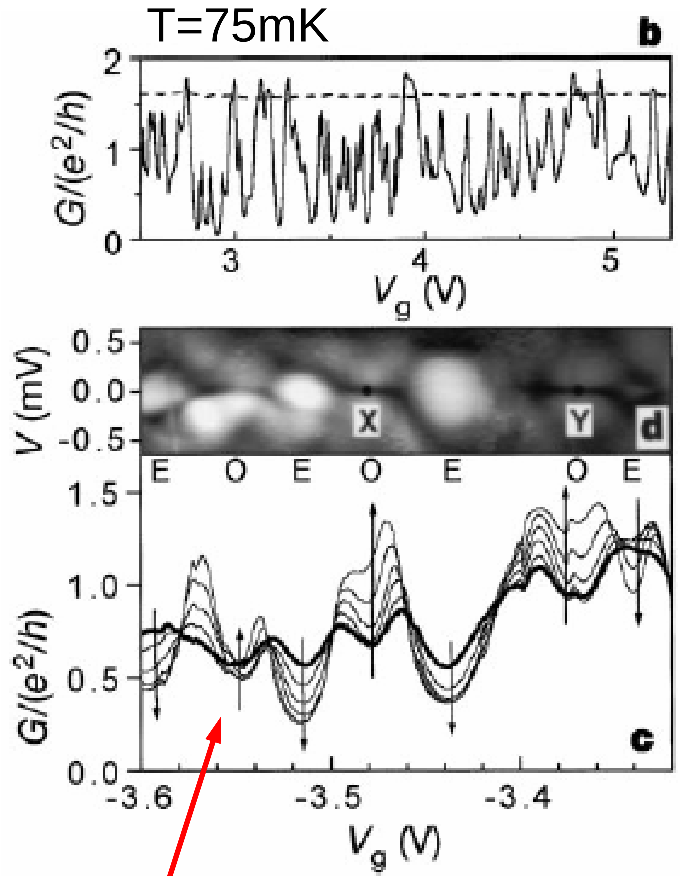

G fluctuates as V_g is swept.

(a darker region represents a higher G)

(T= 75, 125, 180, 245, 320, 490, 560, 780 mk)

LogT dependence of Kondo resonance

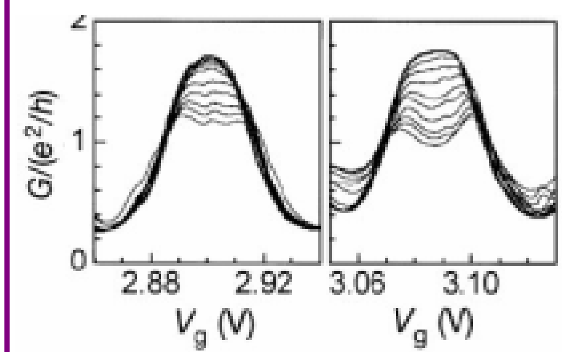

$$G(T) = G_0 \left(\frac{1}{1 + (2^{1/S} - 1)\ T^2 / T_K^2} \right)^S$$

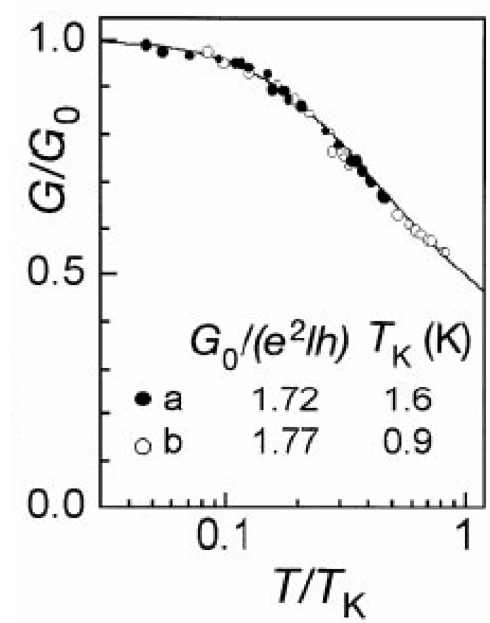

T_K, s : fitting parameters

A generic Kondo effect for even-N quantum dot

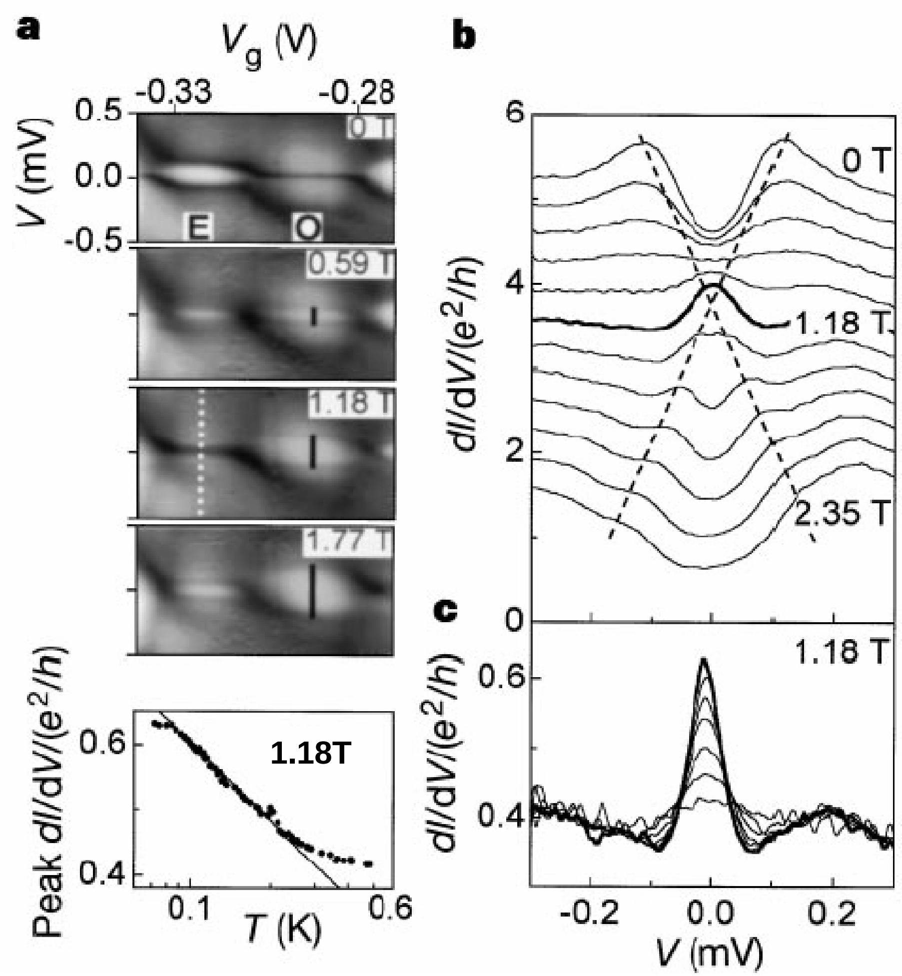

Real Kondo resonance (O)

At V_g= -0.295V

=> Peak splits by $2g\mu_B B/e$.

Generic Kondo resonance

At V_g= -0.322V

Kondo-like effect at B= 1.18T

The dashed line shows $g\mu_B B/e$ slope.

=> Peak splitting follows Zeeman splitting

Log T dependence of the dI/dV peak

Kondo-like resonance

Spin-flipping higher order transitions in a magnetic field

Pustilnik et al., PRL 84, 1756 (2000)

At B=0, ground state is a singlet(S=0).

A triplet(S=1) state is $\Delta_{t\text{-}s}$ above the ground state.

At a certain B, singlet |0,0>와 triplet |1,-1> are in degeneracy.

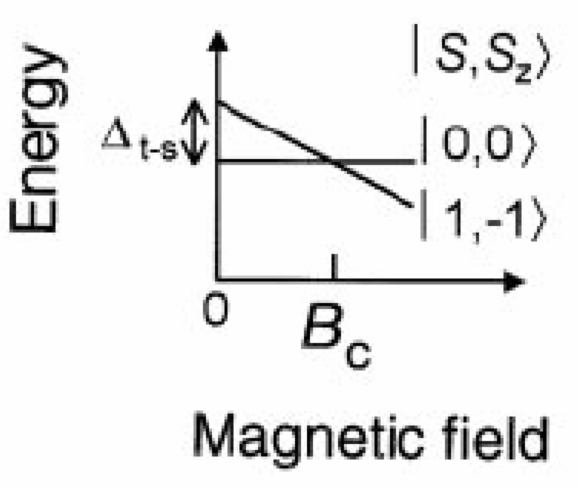

Singlet-triplet alternation

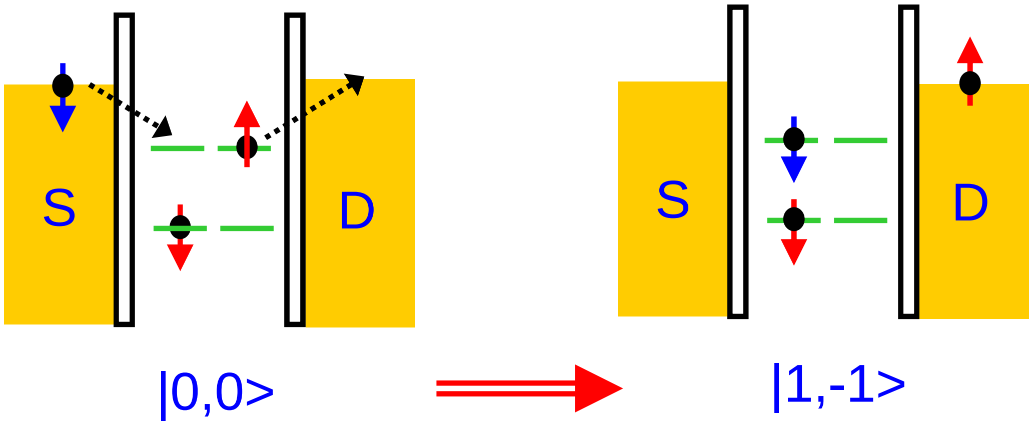

Spin-flipping occurs as electrons co-tunnel, leading a generic Kondo resonance.

Co cluster on a single-walled Carbon Nanotube

Odom et al., Science 290, 1549 (2000)

Co was thermally evaporated onto single walled-CNT.

STM spectroscopic measurements at T= 5K

Apply V between STM tip and single walled-CNT, and measure I or dI/dV.

=> Spectral density of energy state

Kondo resonance was observed.

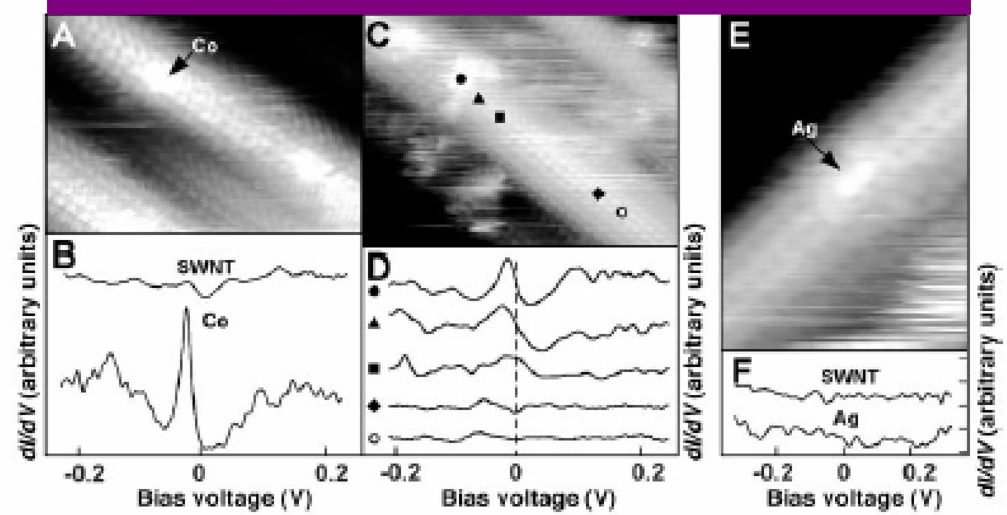

Fig. 1. STM topographic images and spectroscopic measurements on small clusters situated on SWNTs. (A) Atomically resolved image of 0.5-nm Co clusters on an individual nanotube. (B)

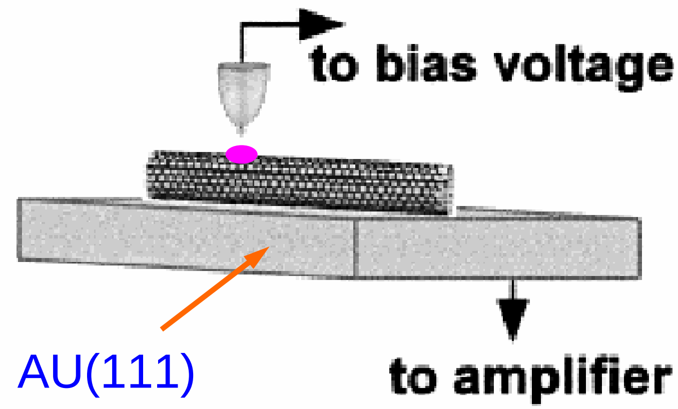

Fabrication

- Spin coating nanotube suspensions of dichloroethane
- Co was thermally evaporated onto SWNT in situ at low temperature

Fano model

Fano, Phys. Rev. 124, 1866 (1961)

Two possible channels

STM tip

d-orbital state of Co magnetic impurity

Continuum state of nanotube

Fano's model (the U= 0 case of the Anderson model) describes this situation.

Asymmetric peak shape

Transition rate in Fano model

$$R(\varepsilon) = R_0(\varepsilon)\frac{(q+\varepsilon')^2}{1+\varepsilon'^2} \quad where \quad \varepsilon' = \frac{\varepsilon-\varepsilon_0}{kT_K}$$

ε_0 는 resonance energy를 나타내고, $R_0(e)$는 transition rate in the absence of discrete state (d-orbital state)를 나타낸다.

q ("interference parameter") $\propto \dfrac{transition \quad amplitude \quad to \quad (d-orbital)}{transition \quad amplitude \quad to \quad (continuum\ state)}$

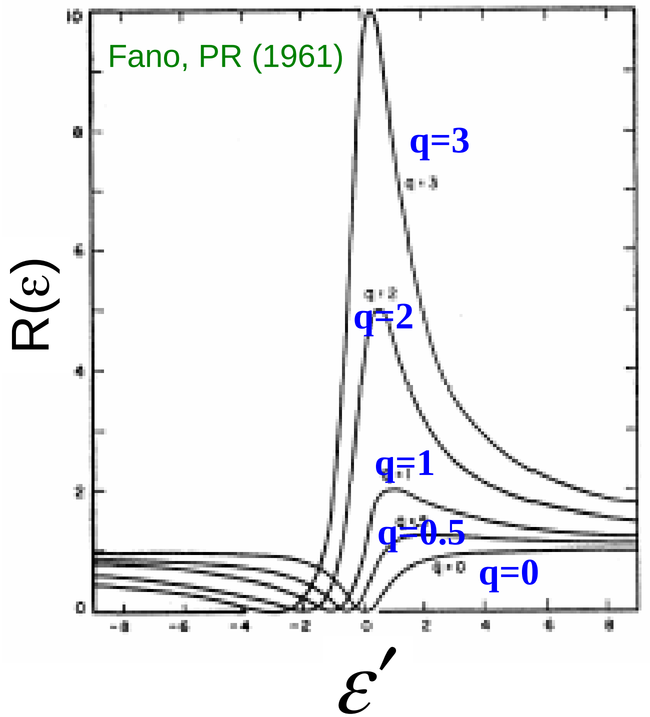

dI/dV spectrum of Co on SWNT

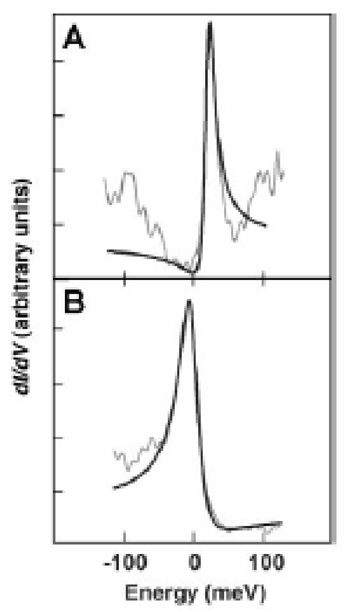

Co size ~ 0.5 nm

$q = 2.7, \ T_K = 93K$

Co size ~ 0.7 nm

$q = -3.3, \ T_K = 185K$

In AuCo bulk, T_K ~ 300 to 700 K

Co cluster on a Au(111) surface

Madhavan et al., Science 280, 567 (1998)

Co was thermally evaporated onto Au(111) surface.

STM spectroscopic measurements at T= 4K.

Kondo resonance was observed, and the shape of the Kondo peak can be explained by Fano's formalism.

STM spectroscopy

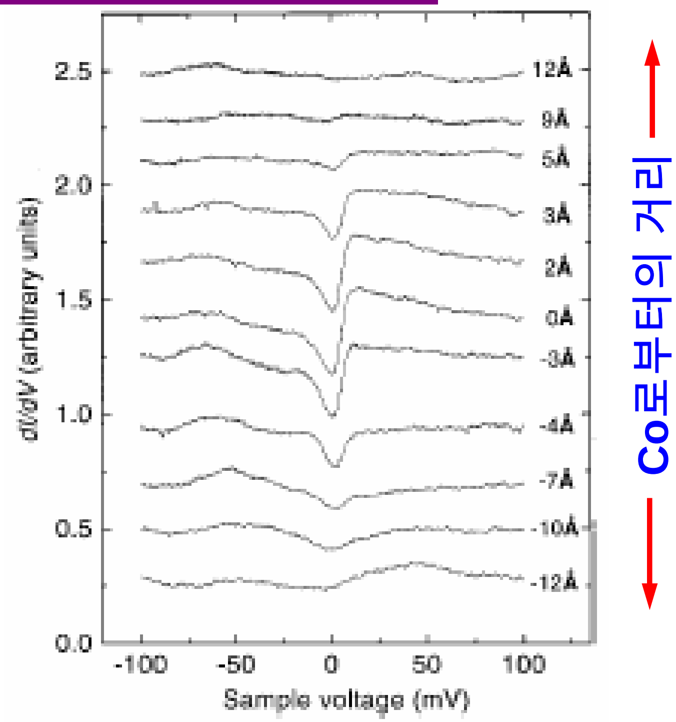

A similar situation as Co on SWNT except for the continuum state
: Au single crystal

$q = 0.7$, $T_K = 64K$

In general, |q| is smaller than that of Co on SWNT.

Co cluster on a SWNT quantum box

Odom et al., Science 290, 1549 (2000)

Using a voltage pulse (7V and 100μs), SWNT was cut into a segment.

Energy level spacing

$$\delta E = \frac{\hbar^2 k_F}{m} \Delta k$$

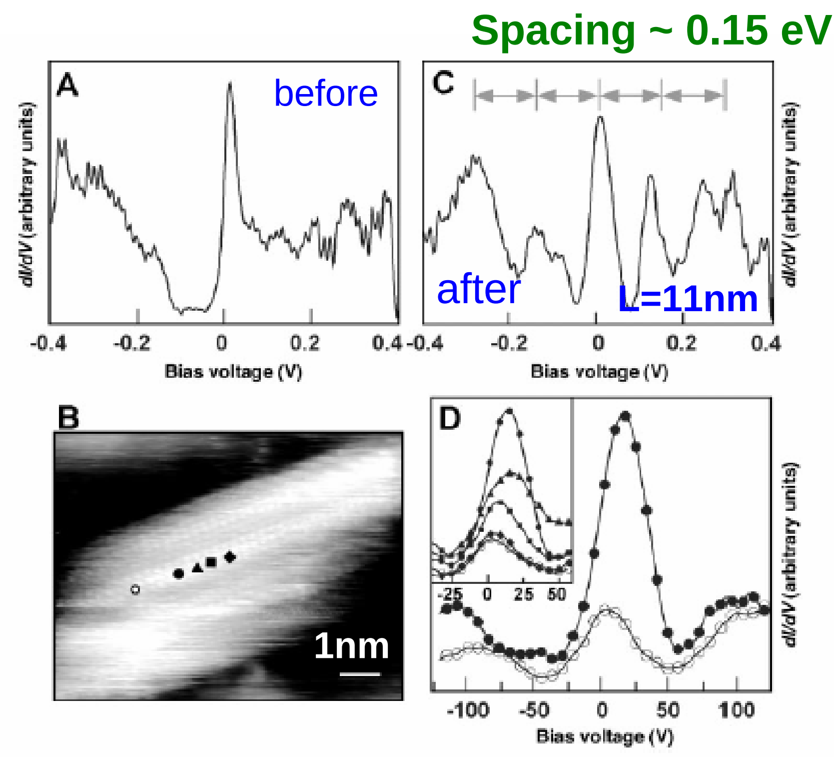

For 1D particle in a box potential, $\Delta k = \pi/L$

$$\delta E = \frac{h\upsilon_F}{2L} \approx \frac{1.67}{L\ [nm]}\ eV$$

,where υ_F is the Fermi velocity of graphene.

Kondo effect in a single molecule transistor

Jiwoong Park et al., Nature 417, 722 (2002)

Molecule $[Co(tpy\text{-}(CH_2)_5\text{-}SH)_2]^{2+}$ or $[Co(tpy\text{-}SH)_2]^{2+}$ where typ: erpyridinyl

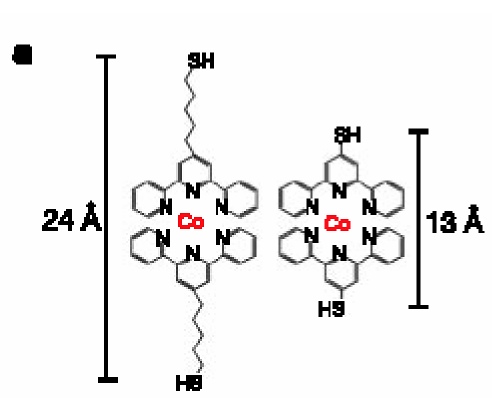

=> Co ion + Linker molecule with different lengths

Fabrication

Continuous Au nanowire (w= 10-15nm, L= 200-400nm).

⇒ A self-assembled monolayer on the Au wire.

⇒ Apply dc voltage (~0.5V) to break the Au wire by electromigration.

This produces a gap about 1-2 nm-wide.

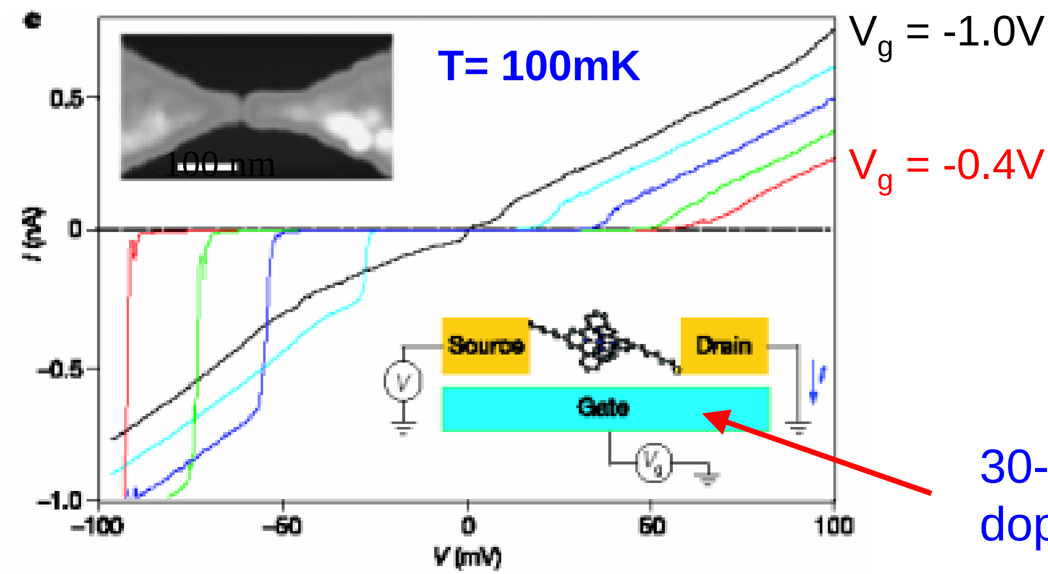

I-V reflects the property of a single electron transistor

30-nm SiO_2 layer on degenerately doped Si Substrate: gate electrode

Recall [Coulomb blockade oscillation]

Kastner, Phys. Today 24 (Jan 1993)

Electrostatic energy of a charge Q on the dot

$$E = QV_g + \frac{Q^2}{2C} = \frac{1}{2C}(Q + CV_g)^2 - CV_g^2$$

Q = …. , -(N+1)e, -Ne, -(N-1)e, ….

$Q_0 = -CV_g$

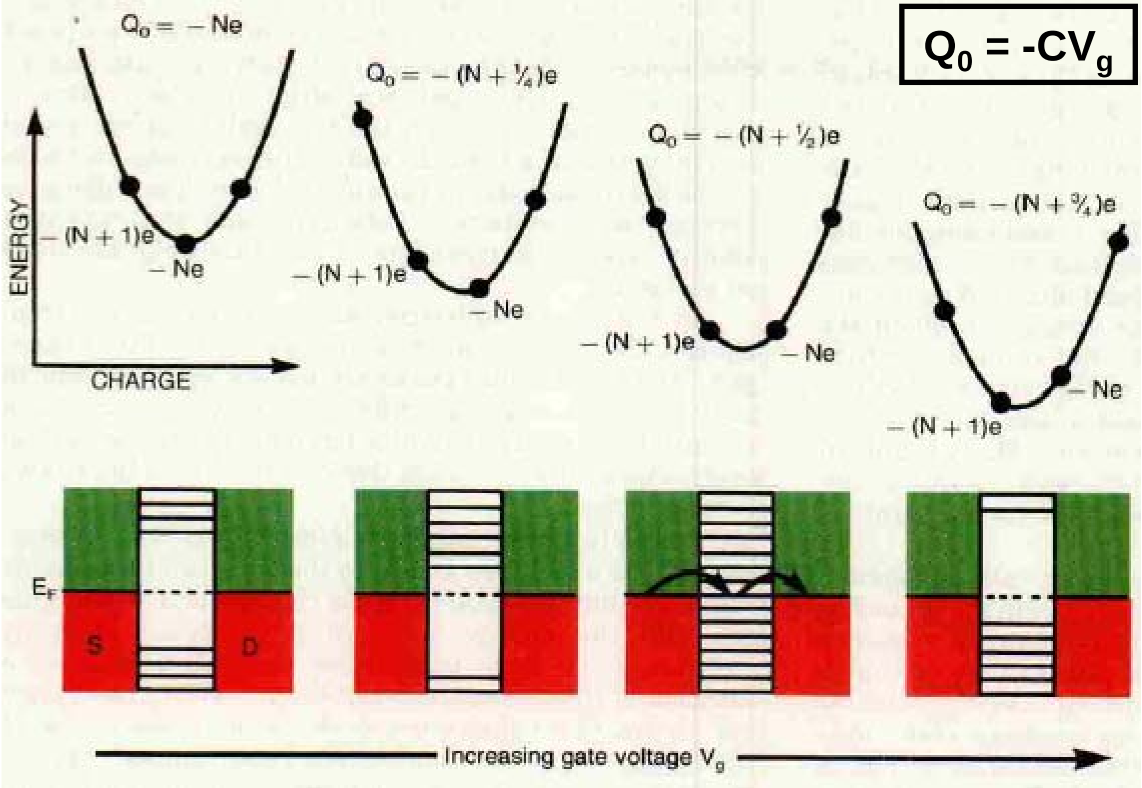

Differential conductance (dI/dV) of single molecule transistor

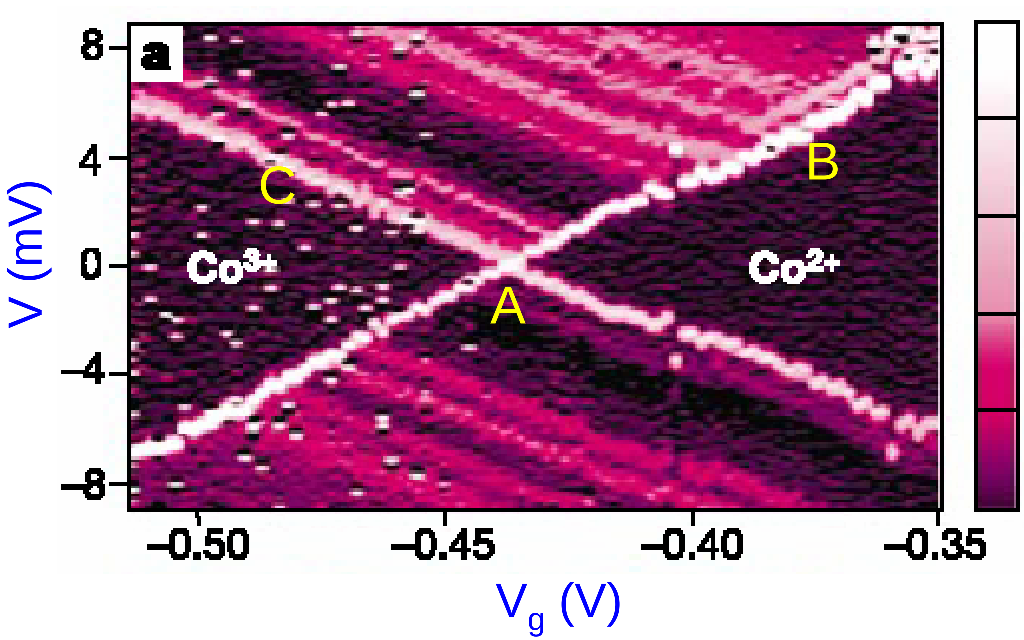

Co ion works as a quantum dot in SET

; No such behavior has been found without Co ion

Energy of a quantum dot

$$E = QV_g + \frac{Q^2}{2C} = \frac{1}{2C}(Q + CV_g)^2 - CV_g^2$$

(A) V = 0

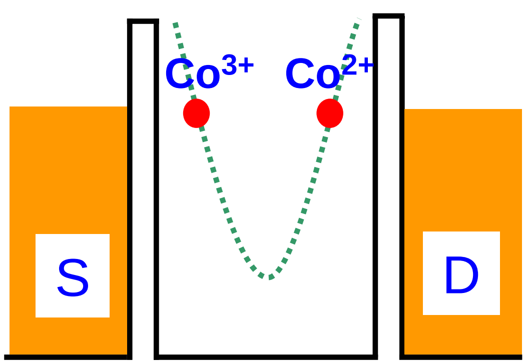

Co^{3+} and Co^{2+} degenerate

(B) V > 0

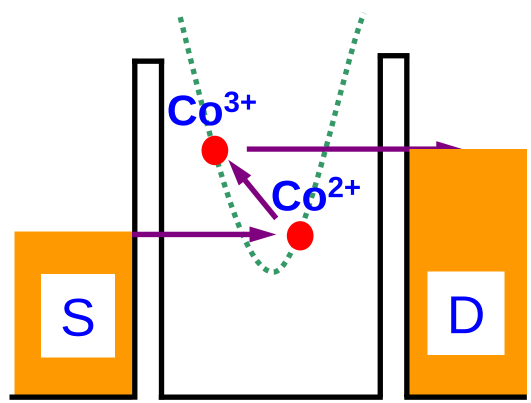

Co^{2+} to Co^{3+} transition

(C) V > 0

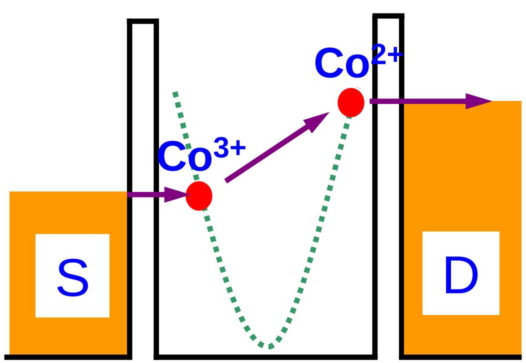

Co^{3+} to Co^{2+} transition

Kondo effect out of equilibrium

Meir et al., PRL 70, 2601 (1993)

"Kondo effect in a voltage bias" was studied through the Anderson Hamiltonian using perturbation theory, noncrossing approximation, equation of motion, variational wave-function calculation methods.

Results

1. A voltage bias causes the Kondo peak to split.

   => A peak in the density of states at the chemical potential of each lead.

2. In a magnetic field, the Kondo peaks shift away from the chemical potentials by Zeeman splitting $\Delta = g\mu_B B$.

   => Kondo peaks shift down for up-spin channel.
   Kondo peaks shift up for down-spin channel.

Kondo peak splitting in a magnetic field

Density of state of an Anderson impurity

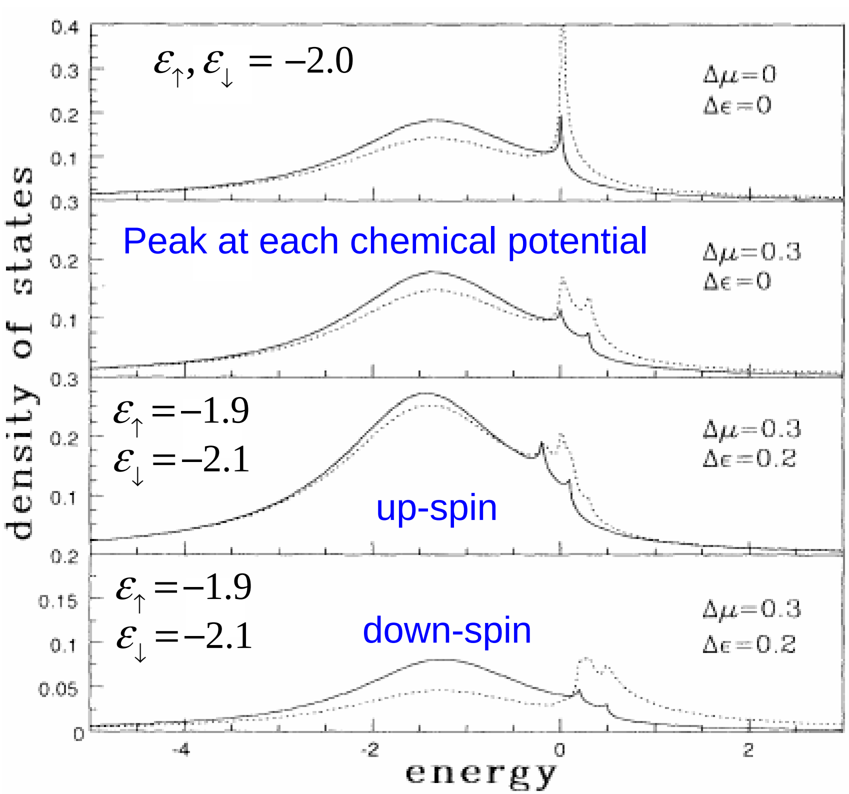

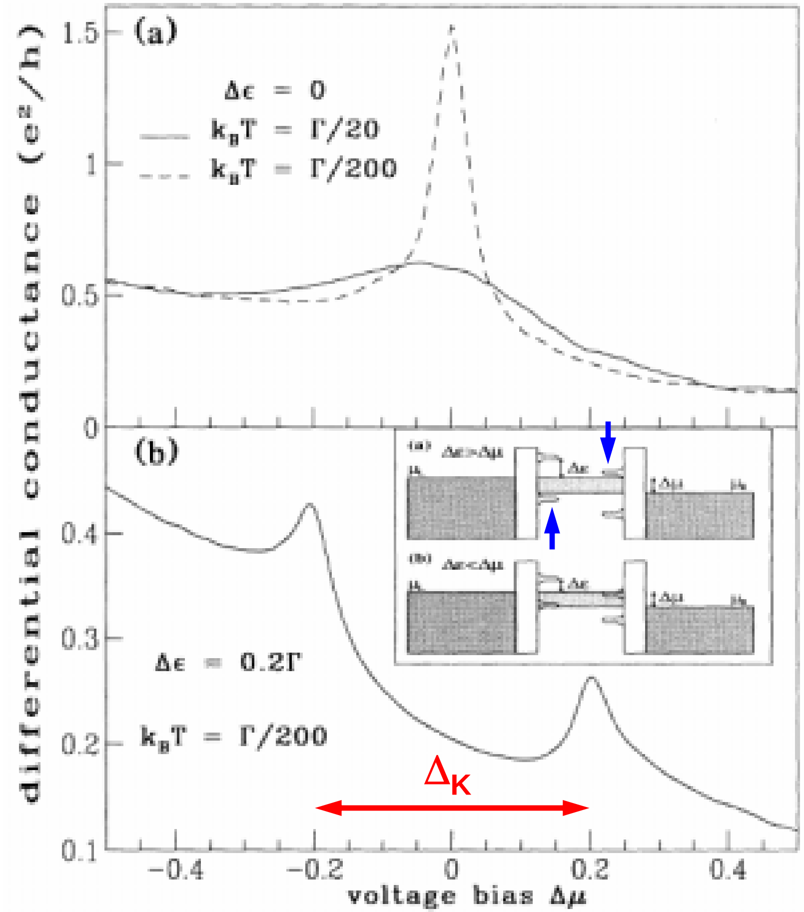

Kondo peak splitting Δ_K is twice the ordinary Zeeman splitting.

$$\boxed{\Delta_K = 2g\mu_B B}$$

Magnetic field dependence of the single molecule transistor

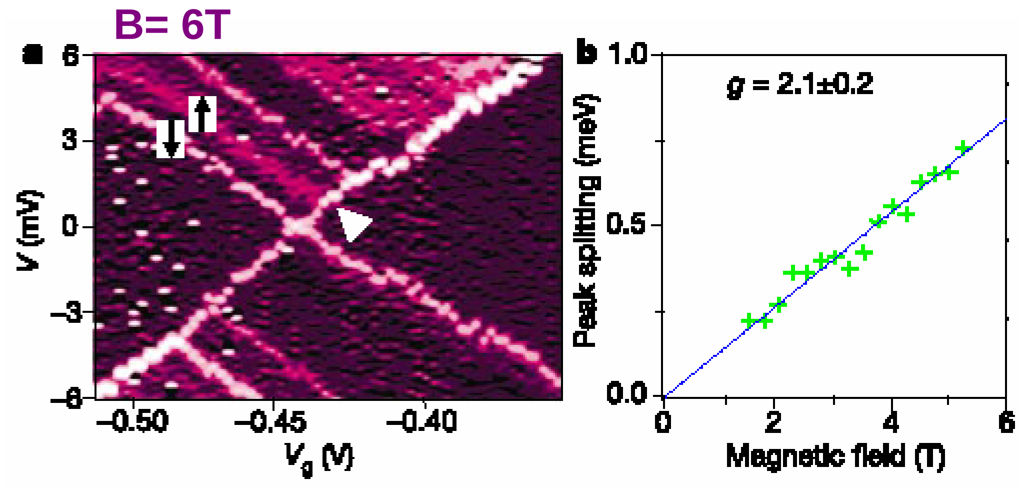

Co^{2+} ion ($3d^7$) : odd number of e
S = 1/2

Co^{3+} ion ($3d^6$) : even number of e
S = 0

Zeeman splitting

$$\Delta = g\mu_B H$$

Kondo resonance for a SMT of $[Co(tpy\text{-}SH)_2]^{2+}$

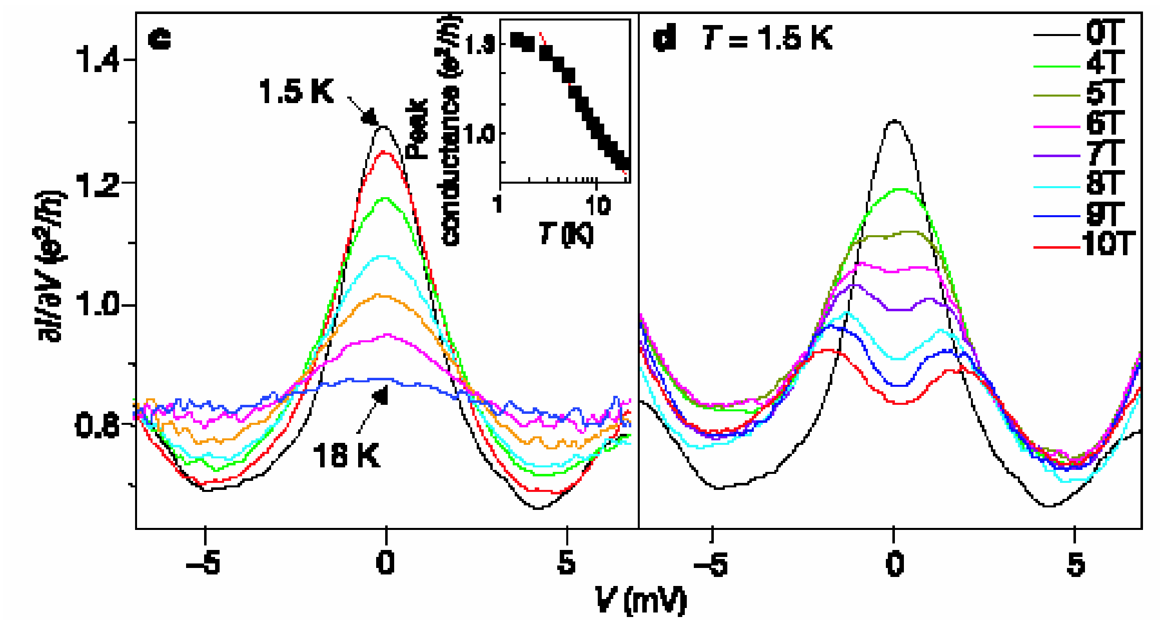

LogT dependence of the Kondo peak

Kondo peak splitting varies linearly with H

$$\Delta_K = 2g\mu_B H$$
$$(g \approx 2)$$

Single-molecule transistor of an individual V_2 molecule

spin impurity

Liang et al., Nature 417, 725 (2002)

[(N,N',N" -trimethyl-1,4,7-triazacyclononane)$_2$-$V_2(CN)_4(\mu\text{-}C_4N_4)$] => V_2 molecule

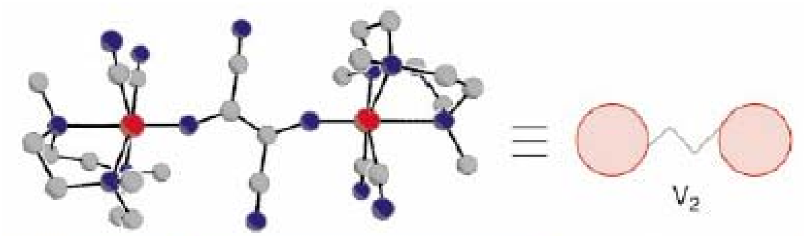

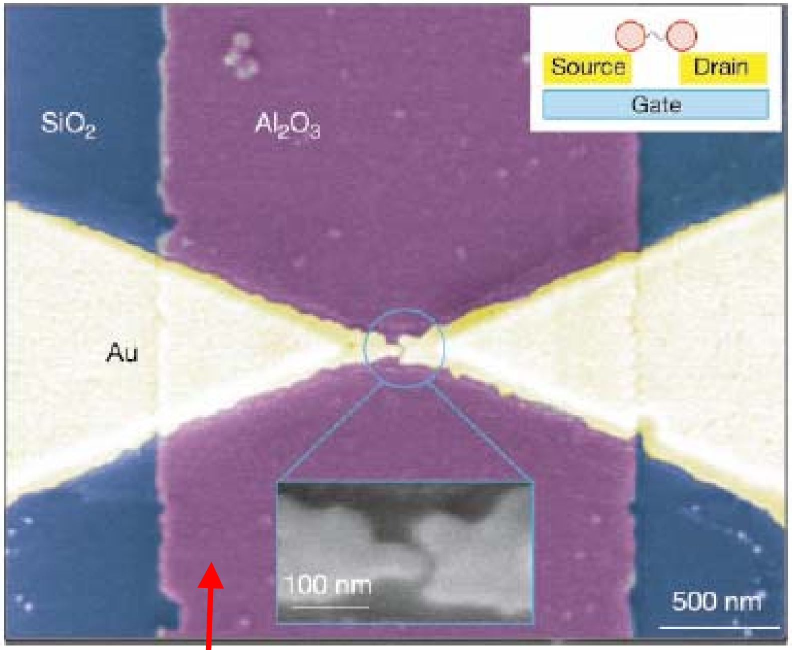

3-nm oxide Al layer: gate electrode

Fabrication

Electromigration-induced break-junction technique

Gap between two electrode is ~ 1 nm.

Differential conductance dI/dV of V_2 transistor

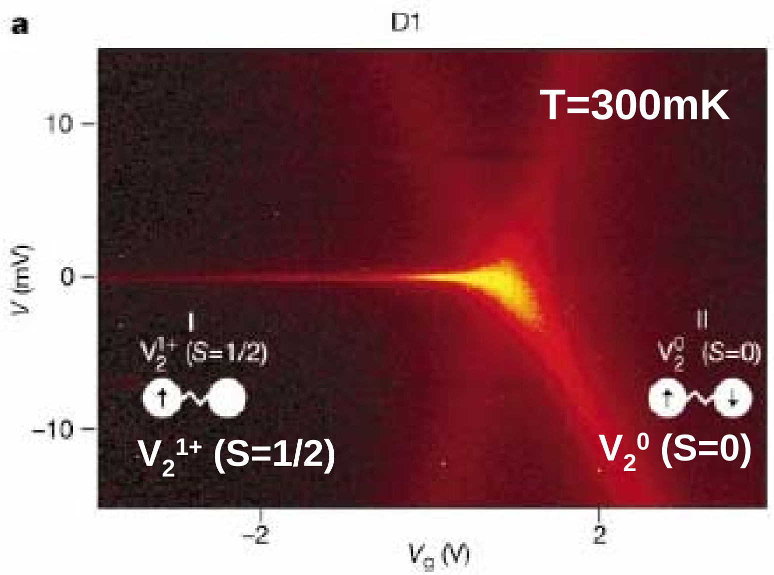

Scale: Dark red(0) to bright yellow($1.55e^2/h$)

SET characteristic was observed.

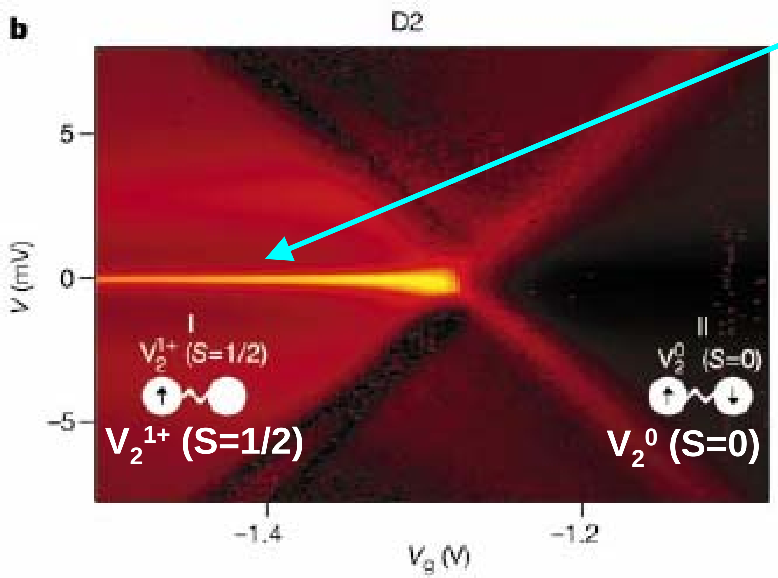

Kondo resonance peak at V_2^{1+} state

Only appears when the molecule has non-zero spin.

Magnetic field dependence

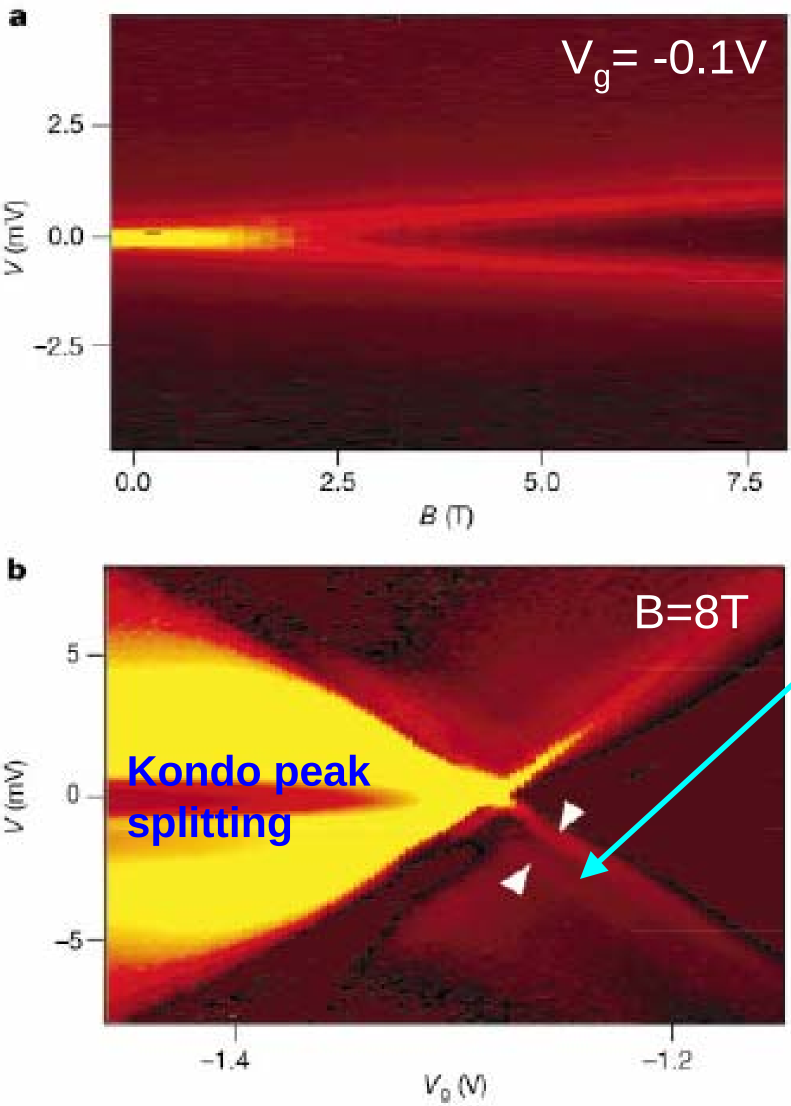

Splitting of Kondo peak

$$\Delta_K = 2g\mu_B B$$

Twice the ordinary Zeeman splitting

$$(\mu_B \approx 58 \ \mu eV / T)$$

From experiment

$$\frac{\Delta_K}{eB} = \frac{e \ \delta V_K}{B} \approx 230 \ \mu eV / T$$

Zeeman splitting

From experiment

$$\frac{\Delta}{eB} = \frac{e \ \delta V}{B} \approx 115 \ \mu eV / T$$

Temperature dependence of Kondo peak

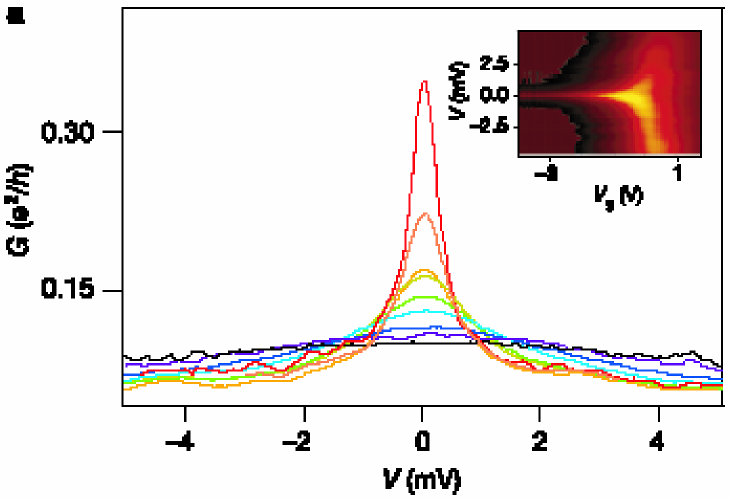

Kondo peak at
T = 0.3, 1.0, 2.0, 3.1, 4.2, 6.3, 9.0, 14, 20 K.
(V_g was set to -2.25V)

For each ε/Γ, the Kondo peak $G_K(T)$ were plotted.

Inset : $G_K(T)$ at ε/Γ = 0.43

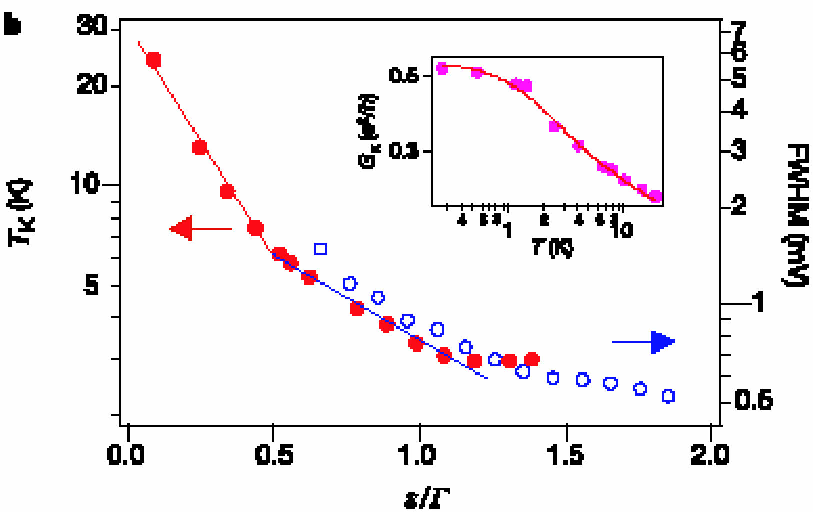

Fit to the empirical formula

$$G_K(T) = G_0 \left(\frac{1}{1 + (2^{1/S} - 1)\ T^2 / T_K^2} \right)^S$$

Fitting yields T_K = 12.2 K and s = 0.19

ε : energy of the localized electron ($\varepsilon = \alpha e V_g$ + const)

Γ : level width due to the coupling to the electrodes